Densities and Thermal Expansion of Some Aqueous Rare Earth Chloride Solutions Between 5° and 80°C. II. $SmCl_3$, $GdCl_3$, $DyCl_3$, $ErCl_3$, and $YbCl_3$

Anton Habenschuss and Frank H. Spedding[1]

Ames Laboratory-ERDA and Department of Chemistry, Iowa State University, Ames, Iowa 50010

A dilatometric method is used to determine the densities of aqueous solutions of $SmCl_3$, $GdCl_3$, $DyCl_3$, $ErCl_3$, and $YbCl_3$ from approximately 0.1 to 3.5 molal, and from 5° to 80°C at 5° intervals. Temperature and concentration dependent empirical equations representing the apparent molal volumes are given. The partial molal volumes, coefficients of thermal expansion, and apparent and partial molal expansibilities derived from these fits are discussed in terms of the ion-ion and ion-solvent interactions in these solutions and their dependence on ion size. The previously reported two-series effect in the apparent and partial molal volume properties at 25°C across the rare earth series, although modified, persists from 5° to 80°C at all concentrations. The coefficients of thermal expansion and apparent and partial molal expansibilities increase with decreasing ionic radius of the rare earth cation, with a reversal in this trend in the middle of the rare earth series.

Recently, we have reported thermal expansion data on aqueous solutions of three light rare earth chlorides (*4*). The thermal expansion data for solutions containing trivalent rare earth ions are consistent with the behavior of solutions of divalent and monovalent cations, i.e., with respect to increasing charge on the cation. However, the thermal expansion properties of solutions containing trivalent rare earth ions were tentatively found to increase with decreasing cationic radius, a trend which is opposite the trend expected from simple surface charge density arguments. This conclusion was based on a very small range in radii, ~0.07 Å (La to Nd).

In this report we extend these measurements to representative members of the remaining rare earth series, covering a 0.2 Å range in radius, to see if this trend holds across the rare earth series. Since anomalies attributed to a decrease in inner sphere water coordination of the rare earth cations between Nd and Tb are prevalent in most thermodynamic and transport properties of rare earth solutions, it was also of interest to see if such a two-series effect was present in the thermal expansion of these solutions across the rare earth series. With these considerations in mind, the measurements reported on $LaCl_3$, $PrCl_3$, and $NdCl_3$ solutions (*4*) have been extended to $SmCl_3$, $GdCl_3$, $DyCl_3$, $ErCl_3$, and $YbCl_3$ solutions.

Experimental

The densities were determined with mercury displacement dilatometers similar to those described by Owen et al. (*11*). The apparatus and procedure have been fully described (*3, 4*). The dilatometers were calibrated with mercury and water, and for solution runs the dilatometers contained about 25 ml of mercury and about 100 ml of degassed solution. The densities were determined at 5°C intervals from 5° to 80°C. Density changes with temperature of less than ±1 ppm and absolute densities of ±5 to 10 ppm could be determined.

[1] To whom correspondence should be addressed.

The stock solutions were prepared by the method of Spedding et al. (*15*), which results in solutions of the stoichiometric salt. Secondary solutions were prepared by dilution with conductivity water. Due to a small loss of water when the solutions were degassed, the concentrations of the solutions were obtained from the measured densities at 25.000°C and existing 25°C pycnometric density data (*18*), rather than by preparing the dilutions by weight. The concentrations obtained in this way were checked with EDTA weight titrations (*14*) for several dilutions. The agreement was within ±0.1% in terms of the molality.

Calculations and Results

The experimental temperatures and densities are given in Tables I–V. The densities were fitted as a function of temperature to

$$d = \sum_{i=0}^{5} C_i t^i \tag{1}$$

for each solution. The coefficients in Equation 1 are given in Table VI, and the deviations from the experimental densities are given in Tables I–V. The concentration of each solution was obtained from the density at 25.000°C as computed from Equation 1 and the pycnometric density data of Spedding et al. (*18*).

The apparent molal volumes were calculated from

$$\phi_V = \frac{1000(d^\circ - d)}{m d^\circ d} + \frac{M_2}{d} \tag{2}$$

at each temperature, where m is the molality, M_2 is the molecular weight of the salt (1969 IUPAC atomic weights), and d° was taken from Gildseth et al. (*3, 4*). The apparent molal volumes are listed in Tables I–V. To represent the apparent molal volumes analytically, they were fitted as a function of temperature to

$$\phi_V = \sum_{i=0}^{5} A_i t^i \tag{3}$$

at each concentration. The coefficients are given in Table VII, and the deviations in Tables I–V. The coefficients in Equation 3 were then fitted as a function of concentration resulting in

$$\phi_V = \sum_i \sum_j B_{ij} m^{j/2} t^i \tag{4}$$

The matrix coefficients, B_{ij}, are given in Table VIII. Equation 4 fits the experimental ϕ_V data to within 0.05 ml/mol at low concentrations and to within 0.01 ml/mol at high concentrations.

From Equation 4 and standard relationships (*4, 6*), the partial molal volume of the solute, $\bar{V}_2$, and the solvent, $\bar{V}_1$, the apparent molal expansibility, ϕ_E, the partial molal expansibility of the solute, $\bar{E}_2$, and the solvent, $\bar{E}_1$, and the coefficient of thermal expansion, α, were calculated at even temperatures and concentrations.

In addition to the empirical approach in the data treatment just outlined, the data were also analyzed in terms of the em-

Table I. Density and ϕ_V for $SmCl_3$

t, °C	d, g/ml	$\Delta d \times 10^6$	ϕ_V, ml/mol	$\Delta\phi_V \times 10^3$
		0.098490m		
5.045	1.023959	−0.9	13.041	−2.1
10.012	1.023559	1.7	14.336	4.3
15.015	1.022846	0.5	15.316	−0.6
20.046	1.021851	−1.1	16.040	−0.3
24.878	1.020661	−0.9	16.517	−4.6
30.012	1.019166	−0.8	16.840	3.7
34.878	1.017549	1.0	16.969	−3.5
40.032	1.015639	1.1	16.966	1.5
44.967	1.013633	0.4	16.830	5.5
49.911	1.011462	0.3	16.562	−2.5
54.903	1.009113	−0.9	16.189	1.2
60.425	1.006343	−1.1	15.643	−0.2
63.783	1.004575	0.2	15.239	−8.9
70.139	1.001058	−0.0	14.384	8.9
75.036	0.998206	1.5	13.595	−1.2
79.388	0.995568	−0.8	12.829	−1.1
		0.23601m		
5.045	1.056895	0.1	14.764	−4.9
10.012	1.056302	−0.6	16.031	11.2
15.015	1.055434	1.1	16.982	−2.3
20.046	1.054307	−0.4	17.698	−3.3
24.878	1.053012	0.2	18.180	−6.5
30.012	1.051424	−0.5	18.517	−0.0
34.878	1.049734	−0.9	18.683	6.4
40.032	1.047763	0.8	18.703	2.0
44.967	1.045710	0.7	18.601	1.0
49.911	1.043502	0.6	18.384	−2.1
54.903	1.041126	−0.8	18.062	−0.3
60.425	1.038335	−1.6	17.586	2.1
63.783	1.036561	1.3	17.227	−8.5
70.139	1.033037	−0.1	16.463	4.2
75.036	1.030187	0.4	15.767	4.3
79.388	1.027559	−0.2	15.077	−3.2
		0.40942m		
5.045	1.097678	−0.2	16.498	−2.2
10.012	1.096857	0.2	17.692	4.6
15.015	1.095794	−0.4	18.610	2.0
20.046	1.094511	3.3	19.288	−10.2
24.878	1.093078	−4.3	19.778	6.4
30.012	1.091379	−0.5	20.101	−0.1
34.878	1.089599	1.3	20.270	−1.5
40.032	1.087545	1.3	20.318	−0.1
44.967	1.085427	0.8	20.248	0.5
49.911	1.083165	−1.1	20.075	2.7
54.903	1.080747	−1.2	19.799	0.7
60.425	1.077922	0.1	19.382	−3.1
63.783	1.076129	−0.0	19.078	−1.7
70.139	1.072586	1.3	18.397	−0.8
75.036	1.069726	−0.8	17.788	5.4
79.388	1.067097	0.1	17.174	−2.7
		0.59909m		
5.045	1.141387	0.1	18.125	−2.1
10.012	1.140338	−0.4	19.236	4.2
15.015	1.139080	0.4	20.098	0.2
20.046	1.137622	0.1	20.754	−2.1
24.878	1.136056	−0.2	21.214	−2.1
30.012	1.134225	−0.2	21.544	−0.5
34.878	1.132341	0.8	21.722	−0.1
40.032	1.130194	−1.0	21.790	3.6
44.967	1.128004	0.1	21.741	1.4
49.911	1.125682	0.6	21.594	−0.7
54.903	1.123213	−0.0	21.356	−1.4
60.425	1.120342	−0.7	20.992	−0.8
63.783	1.118529	0.5	20.720	−2.0
70.139	1.114955	0.1	20.113	1.4
75.036	1.112080	−0.2	19.562	2.7
79.388	1.109442	0.1	19.012	−1.8
		0.79726m		
5.045	1.186115	−0.0	19.604	−1.4
10.012	1.184843	0.0	20.640	2.6
15.015	1.183389	0.0	21.452	0.5
20.046	1.181764	0.3	22.074	−1.8
24.878	1.180056	−0.6	22.515	−1.1
30.012	1.178097	−0.1	22.836	−0.5
34.878	1.176107	0.2	23.018	0.6
40.032	1.173864	0.2	23.095	1.3
44.967	1.171594	0.4	23.066	0.8
49.911	1.169204	−0.6	22.947	0.8
54.903	1.166677	−0.1	22.740	−1.0
60.425	1.163754	−0.1	22.418	−1.3
63.783	1.161913	0.5	22.177	−1.4
70.139	1.158298	−0.3	21.632	1.4
75.036	1.155401	0.1	21.135	1.7
79.388	1.152746	−0.0	20.639	−1.2
		1.0194m		
5.045	1.235151	−0.1	21.068	−1.0
10.012	1.233648	0.2	22.030	1.9
15.015	1.231989	−0.0	22.791	0.5
20.046	1.230183	−0.5	23.379	−0.8
24.878	1.228325	0.5	23.798	−1.7
30.012	1.226223	−0.0	24.112	−0.4
34.878	1.224114	−0.1	24.295	0.7
40.032	1.221763	−0.3	24.381	1.4
44.967	1.219403	0.2	24.369	0.8
49.911	1.216935	0.5	24.272	−0.3
54.903	1.214339	−0.2	24.095	−0.6
60.425	1.211352	−1.1	23.813	−0.2
63.783	1.209479	1.1	23.597	−1.6
70.139	1.205811	−0.3	23.109	1.1
75.036	1.202882	0.1	22.662	1.3
79.388	1.200204	−0.0	22.214	−0.9
		1.2623m		
5.045	1.287475	0.1	22.501	−0.9
10.012	1.285738	−0.3	23.392	1.8
15.015	1.283870	0.0	24.103	0.4
20.046	1.281875	0.4	24.657	−1.2
24.878	1.279854	−0.3	25.060	−0.9
30.012	1.277598	−0.4	25.365	−0.1
34.878	1.275361	0.6	25.549	0.1
40.032	1.272887	−0.2	25.646	1.1
44.967	1.270422	−0.1	25.652	0.8
49.911	1.267860	0.1	25.579	0.0
54.903	1.265182	−0.2	25.433	−0.5
60.425	1.262114	−0.2	25.190	−0.8
63.783	1.260196	0.4	25.003	−0.8
70.139	1.256456	0.0	24.573	0.7
75.036	1.253478	−0.3	24.176	1.3
79.388	1.250764	0.1	23.776	−0.9
		1.5089m		
5.045	1.339207	0.2	23.823	−0.8
10.012	1.337246	−0.6	24.654	1.7
15.015	1.335176	0.8	25.322	−0.1
20.046	1.332995	−0.1	25.849	−0.7
24.878	1.330812	−0.4	26.236	−0.7
30.012	1.328401	−0.1	26.535	−0.2
34.878	1.326028	0.4	26.723	0.2
40.032	1.323424	0.5	26.831	0.5
44.967	1.320845	−0.5	26.854	0.9
49.911	1.318182	0.9	26.805	−0.4
54.903	1.315406	−2.7	26.689	0.9
60.425	1.312249	2.4	26.481	−2.0
63.783	1.310277	−0.1	26.321	−0.4
70.139	1.306447	−0.3	25.946	0.7
75.036	1.303407	−0.4	25.596	1.2
79.388	1.300641	0.3	25.243	−0.8
		1.7430m		
5.045	1.387022	0.4	24.990	−0.8
10.012	1.384861	−0.9	25.772	1.6
15.015	1.382606	−0.1	26.406	0.3
20.046	1.380256	1.3	26.909	−1.2
24.878	1.377921	−0.9	27.285	−0.4
30.012	1.375362	0.4	27.579	−0.4
34.878	1.372859	0.2	27.770	0.3
40.032	1.370127	−0.4	27.888	0.9
44.967	1.367436	−0.6	27.927	0.8
49.911	1.364668	0.4	27.898	−0.1
54.903	1.361798	0.3	27.806	−0.6
60.425	1.358536	−0.3	27.635	−0.5
63.783	1.356510	0.5	27.497	−0.6
70.139	1.352580	−0.3	27.170	0.6
75.036	1.349471	−0.2	26.860	0.9
79.388	1.346649	0.2	26.546	−0.7

Table I. Continued

t, °C	d, g/ml	Δd × 10⁶	φV, ml/mol	Δφv × 10³
		2.0041m		
5.045	1.438871	0.4	26.214	−0.7
10.012	1.436502	−1.0	26.948	1.4
15.015	1.434049	0.1	27.548	0.2
20.046	1.431511	1.4	28.030	−1.1
24.878	1.429006	−0.3	28.396	−0.6
30.012	1.426274	−0.9	28.689	0.1
34.878	1.423620	0.0	28.886	0.3
40.032	1.420737	−0.2	29.017	0.7
44.967	1.417910	0.2	29.074	0.4
49.911	1.415013	0.8	29.069	−0.3
54.903	1.412020	−0.3	29.005	−0.3
60.425	1.408632	−0.4	28.870	−0.4
63.783	1.406533	−0.0	28.756	−0.3
70.139	1.402477	0.2	28.479	0.4
75.036	1.399276	0.0	28.212	0.7
79.388	1.396376	−0.0	27.938	−0.5
		2.2697m		
5.073	1.490003	0.2	27.393	−0.6
10.018	1.487442	−0.6	28.083	1.1
15.030	1.484788	0.2	28.655	0.2
20.067	1.482059	0.4	29.120	−0.6
24.896	1.479386	0.1	29.476	−0.6
30.011	1.476493	−0.1	29.766	−0.2
34.910	1.473663	−0.4	29.969	0.4
40.072	1.470620	0.6	30.111	0.4
44.979	1.467666	−0.6	30.184	0.6
49.920	1.464636	0.2	30.200	−0.0
54.920	1.461509	0.4	30.161	−0.5
60.458	1.457975	−0.5	30.057	−0.3
63.783	1.455820	0.4	29.965	−0.5
70.104	1.451646	−0.2	29.734	0.5
75.008	1.448343	−0.0	29.505	0.6
79.400	1.445335	0.0	29.264	−0.4
		2.5663m		
5.073	1.545206	0.1	28.638	−0.5
10.018	1.542435	−0.4	29.286	0.9
15.030	1.539573	0.6	29.831	0.0
20.067	1.536638	−1.1	30.279	−0.2
24.896	1.533777	0.5	30.626	−0.7
30.011	1.530692	1.0	30.915	−0.5
34.910	1.527684	−0.7	31.125	0.5
40.072	1.524464	0.5	31.278	0.3
44.979	1.521348	−1.2	31.367	0.7
49.920	1.518163	0.3	31.402	−0.1
54.920	1.514887	−0.3	31.388	−0.2
60.458	1.511199	1.6	31.315	−0.9
63.783	1.508950	−1.2	31.245	0.1
70.104	1.504617	0.6	31.056	0.2
75.008	1.501196	−0.8	30.864	0.8
79.400	1.498090	0.4	30.656	−0.5
		2.8531m		
5.073	1.596733	0.2	29.782	−0.4
10.018	1.593764	−0.6	30.397	0.9
15.030	1.590709	0.7	30.918	−0.0
20.067	1.587587	−0.4	31.350	−0.3
24.896	1.584550	0.4	31.690	−0.6
30.011	1.581283	−0.1	31.978	−0.1
34.910	1.578108	−0.2	32.191	0.3
40.072	1.574714	0.1	32.354	0.4
44.979	1.571442	−0.2	32.456	0.4
49.920	1.568105	−0.0	32.509	0.0
54.920	1.564682	0.5	32.514	−0.4
60.458	1.560839	0.2	32.467	−0.4
63.783	1.558506	−0.4	32.414	−0.1
70.104	1.554014	−0.3	32.261	0.4
75.008	1.550479	0.5	32.097	0.4
79.400	1.547273	−0.2	31.920	−0.3
		3.1436m		
5.073	1.647026	0.2	30.891	−0.4
10.018	1.643873	−0.1	31.476	0.7
15.030	1.640630	−0.5	31.976	0.2
20.067	1.637326	−0.6	32.394	−0.2
24.896	1.634118	1.3	32.726	−0.7
30.011	1.630673	0.6	33.012	−0.3
34.910	1.627333	−0.6	33.228	0.3
40.072	1.623774	−0.1	33.398	0.4
44.979	1.620350	−1.0	33.509	0.5
49.920	1.616867	−0.4	33.575	0.1
54.920	1.613305	1.7	33.596	−0.6
60.458	1.609313	−0.6	33.570	−0.2
63.783	1.606896	0.3	33.530	−0.3
70.104	1.602254	0.4	33.405	0.2
75.008	1.598610	−1.1	33.267	0.7
79.400	1.595316	0.5	33.111	−0.4
		3.4579m		
5.073	1.699284	0.3	32.059	−0.4
10.018	1.695939	−0.9	32.616	0.8
15.030	1.692508	0.5	33.094	0.0
20.067	1.689017	0.2	33.498	−0.4
24.896	1.685633	−0.2	33.822	−0.4
30.011	1.682014	1.5	34.104	−0.4
34.910	1.678510	−1.0	34.319	0.4
40.072	1.674786	−1.5	34.493	0.6
44.979	1.671214	−1.4	34.611	0.6
49.920	1.667593	3.5	34.686	−0.7
54.920	1.663889	1.0	34.720	−0.5
60.458	1.659752	−2.5	34.711	0.1
63.783[a]	1.657265	9.9	34.680	−2.3
70.104	1.652464	−0.3	34.581	0.2
75.008	1.648718	1.3	34.462	0.1
79.400	1.645333	−0.6	34.327	−0.1

[a] Entry not used in the least-squares fits.

pirical Masson (*8*) and the semiempirical Redlich-Meyer type (*13*) equations. The constants ϕ_V^* and S_V^* in the Masson equation

$$\phi_V = \phi_V^* + S_V^* m^{1/2} \quad (5)$$

are listed in Table IX at even temperatures. These constants serve to relate the results of this study to the numerous existing data (*9*) analyzed in terms of this equation. Obviously, this two-parameter equation is of only qualitative value. The Redlich-Meyer type equation used had the form of Equation 4, where the coefficients in $m^{1/2}$ are fixed to represent the theoretical limiting slope of Debye-Hückel as a function of temperature (*9*). The extrapolation to infinite dilution with this equation is somewhat uncertain due to the absence of ϕ_V data below 0.1*m* at temperatures other than 25°C. However, the extrapolated ϕ_V^0 and ϕ_E^0 from the Redlich-Meyer equation should be more realistic than either the Masson ϕ_V^* or the extrapolation of the completely empirical Equation 4. The ϕ_V^0 and ϕ_E^0 obtained from the Redlich-Meyer extrapolation are listed in Table X where the results for $LaCl_3$, $PrCl_3$, and $NdCl_3$ are also tabulated. The ϕ_V^0 obtained in this way at 25°C agree with the extrapolated ϕ_V^0 from dilute magnetic float data (*14*) to within 0.5 ml/mol. The goodness of fit of the Redlich-Meyer equation in the experimental range was somewhat less than the completely empirical Equation 4, and we have chosen the latter to represent our actual experimental data.

The errors are substantially the same as reported in the earlier measurements (*4*), where they are discussed at length. Briefly, in the density we expect absolute errors of 5–10 ppm, and temperature dependent relative errors of less than 1 ppm; absolute errors in ϕ_V of 0.2 ml/mol at low concentrations to 0.1 ml/mol at high concentrations, and temperature dependent relative errors in ϕ_V of 0.01 ml/mol at low concentrations to 0.0005 ml/mol at high concentrations;

Table II. Density and ϕ_V for $GdCl_3$

t, °C	d, g/ml	$\Delta d \times 10^6$	ϕ_V, ml/mol	$\Delta\phi_V \times 10^3$
		0.097765*m*		
5.075	1.024205	−0.6	15.547	−4.6
10.023	1.023819	1.4	16.710	7.3
15.020	1.023120	−0.3	17.560	7.8
20.068	1.022137	−0.1	18.134	−10.7
24.886	1.020961	−0.4	18.492	−9.8
29.999	1.019484	−0.7	18.695	2.8
34.887	1.017870	0.0	18.723	6.1
40.004	1.015985	0.5	18.606	7.3
44.978	1.013974	0.7	18.359	2.5
49.904	1.011820	0.8	17.993	−7.5
54.829	1.009512	0.1	17.527	−9.7
60.413	1.006719	−2.7	16.897	15.3
64.998	1.004299	0.7	16.231	−12.9
70.116	1.001458	0.1	15.435	6.4
74.557	0.998884	1.2	14.636	1.5
79.425	0.995948	−0.7	13.673	−1.9
		0.23685*m*		
5.075	1.058093	−0.5	17.288	−2.5
10.023	1.057539	0.8	18.393	5.5
15.020	1.056702	0.5	19.211	−0.1
20.068	1.055604	−0.3	19.795	−3.6
24.886	1.054338	−1.2	20.164	−0.9
29.999	1.052786	−0.0	20.375	−1.8
34.887	1.051113	0.3	20.433	1.3
40.004	1.049178	0.3	20.357	4.0
44.978	1.047132	0.3	20.160	2.8
49.904	1.044951	0.5	19.853	−1.5
54.829	1.042627	0.6	19.446	−6.0
60.413	1.039824	−1.6	18.881	1.6
64.998	1.037400	−0.6	18.321	0.3
70.116	1.034564	0.3	17.609	2.0
74.557	1.031999	1.5	16.914	−0.4
79.425	1.029076	−0.8	16.082	−0.5
		0.41052*m*		
5.075	1.099652	0.1	18.952	−2.9
10.023	1.098896	−0.2	19.997	5.5
15.020	1.097893	−0.4	20.776	2.0
20.068	1.096657	0.5	21.334	−4.0
24.886	1.095285	2.0	21.687	−7.8
29.999	1.093632	−2.7	21.915	4.9
34.887	1.091887	−0.8	21.980	3.4
40.004	1.089893	0.7	21.922	1.5
44.978	1.087799	1.0	21.753	−0.1
49.904	1.085584	1.3	21.484	−2.8
54.829	1.083232	−1.1	21.127	0.4
60.413	1.080414	−1.1	20.611	−0.3
64.998	1.077983	0.0	20.105	−1.4
70.116	1.075148	0.7	19.460	0.4
74.557	1.072588	0.3	18.836	2.8
79.425	1.069678	−0.3	18.078	−1.5
		0.58944*m*		
5.075	1.141614	0.3	20.443	−2.3
10.023	1.140671	−0.9	21.414	4.9
15.020	1.139511	0.7	22.143	−0.2
20.068	1.138139	−0.1	22.676	−1.8
24.886	1.136657	−0.0	23.020	−2.3
29.999	1.134913	0.2	23.233	−1.0
34.887	1.133091	0.1	23.309	0.9
40.004	1.131031	0.2	23.268	1.8
44.978	1.128886	−1.3	23.123	3.6
49.904	1.126634	0.6	22.880	−0.8
54.829	1.124257	0.7	22.550	−2.6
60.413	1.121415	−0.8	22.081	−0.8
64.998	1.118975	0.5	21.616	−1.7
70.116	1.116135	0.3	21.025	0.8
74.557	1.113577	−0.7	20.450	3.6
79.425	1.110677	0.3	19.750	−2.0
		0.78425*m*		
5.075	1.186386	0.6	21.858	−2.0
10.023	1.185250	−1.4	22.763	4.2
15.020	1.183927	0.2	23.448	0.4
20.068	1.182417	1.4	23.949	−3.0
24.886	1.180821	−0.5	24.279	−1.2
29.999	1.178976	−0.4	24.487	−0.1
34.887	1.177074	0.1	24.567	0.7
40.004	1.174943	0.3	24.538	1.3
44.978	1.172741	−0.6	24.413	1.9
49.904	1.170443	0.0	24.198	0.0
54.829	1.168029	0.2	23.901	−1.3
60.413	1.165159	−0.3	23.474	−1.1
64.998	1.162701	1.1	23.050	−1.9
70.116	1.159850	−0.2	22.510	1.2
74.557	1.157288	−0.9	21.982	2.8
79.425	1.154390	0.4	21.340	−1.7
		0.99472*m*		
5.075	1.233701	0.2	23.227	−1.3
10.023	1.232384	−0.6	24.060	2.6
15.020	1.230899	0.3	24.698	0.2
20.068	1.229248	0.4	25.170	−1.6
24.886	1.227537	−0.2	25.482	−1.2
29.999	1.225585	−0.5	25.684	−0.1
34.887	1.223597	0.2	25.766	0.5
40.004	1.221391	0.8	25.748	0.5
44.978	1.219127	−1.2	25.640	2.0
49.904	1.216779	0.4	25.447	−0.3
54.829	1.214324	0.2	25.180	−1.0
60.413	1.211419	0.0	24.790	−1.2
64.998	1.208939	0.4	24.405	−0.9
70.116	1.206070	−1.2	23.910	1.8
74.557	1.203502	0.9	23.423	0.6
79.425	1.200599	−0.2	22.835	−0.8
		1.2239*m*		
5.075	1.284033	0.8	24.547	−1.5
10.023	1.282527	−2.1	25.319	3.1
15.020	1.280878	0.9	25.913	−0.2
20.068	1.279079	1.1	26.358	−1.7
24.886	1.277244	−1.2	26.656	−0.4
29.999	1.275181	0.6	26.851	−0.8
34.887	1.273098	0.9	26.937	−0.0
40.004	1.270805	−0.2	26.931	1.1
44.978	1.268472	−1.5	26.840	1.8
49.904	1.266064	−0.4	26.671	0.3
54.829	1.263560	−0.2	26.432	−0.6
60.413	1.260610	1.7	26.080	−2.1
64.998	1.258099	1.8	25.731	−1.7
70.116	1.255200	−2.8	25.284	2.6
74.557	1.252617	0.2	24.839	1.0
79.425	1.249704	0.4	24.300	−1.1
		1.4444*m*		
5.075	1.331332	0.4	25.697	−1.0
10.023	1.329658	−0.9	26.418	1.9
15.020	1.327854	−0.0	26.978	0.3
20.068	1.325920	1.2	27.399	−1.5
24.886	1.323970	−0.2	27.685	−0.9
29.999	1.321797	−0.4	27.878	−0.1
34.887	1.319622	−0.3	27.968	0.6
40.004	1.317245	−0.3	27.972	1.0
44.978	1.314841	0.1	27.896	0.6
49.904	1.312370	0.1	27.749	0.0
54.829	1.309814	1.2	27.535	−1.3
60.413	1.306809	−1.0	27.219	−0.3
64.998	1.304265	−0.2	26.900	−0.3
70.116	1.301340	−0.2	26.488	0.7
74.557	1.298734	0.6	26.081	0.6
79.425	1.295800	−0.2	25.586	−0.5
		1.7108*m*		
5.075	1.387010	0.5	26.958	−0.9
10.023	1.385142	−1.2	27.628	1.8
15.020	1.383161	−0.1	28.153	0.3
20.068	1.381065	1.9	28.553	−1.5
24.886	1.378973	−0.5	28.830	−0.6
29.999	1.376664	−0.5	29.022	−0.1
34.887	1.374372	−0.6	29.119	0.7
40.004	1.371887	0.5	29.137	0.5
44.978	1.369387	−0.1	29.081	0.6
49.904	1.366831	−0.2	28.959	0.1
54.829	1.364200	1.1	28.775	−1.0
60.413	1.361120	−1.1	28.498	−0.2
64.998	1.358523	0.4	28.216	−0.5
70.116	1.355545	0.1	27.848	0.4
74.557	1.352896	−0.2	27.485	0.9
79.425	1.349926	0.1	27.040	−0.6

Table II. Continued

t, °C	d, g/ml	Δd × 10⁶	ϕ_V, ml/mol	Δϕ_V × 10³
		1.9407*m*		
5.075	1.433784	0.6	27.959	−0.8
10.023	1.431755	−1.3	28.593	1.6
15.020	1.429624	0.1	29.094	0.2
20.068	1.427388	1.2	29.479	−1.1
24.886	1.425175	−0.1	29.749	−0.7
29.999	1.422746	−0.1	29.942	−0.2
34.887	1.420349	−0.6	30.045	0.6
40.004	1.417763	0.2	30.076	0.6
44.978	1.415174	−0.2	30.037	0.6
49.904	1.412539	0.1	29.936	−0.0
54.829	1.409834	0.3	29.776	−0.6
60.413	1.406681	−0.6	29.530	−0.4
64.998	1.404029	0.7	29.277	−0.6
70.116	1.400996	0.5	28.945	0.2
74.557	1.398304	−1.2	28.615	1.2
79.425	1.395293	0.5	28.209	−0.7
		2.1911*m*		
5.063	1.483408	−0.5	28.972	−0.3
10.001	1.481213	1.4	29.571	0.5
15.009	1.478911	−0.3	30.053	0.3
20.039	1.476529	−1.1	30.426	−0.2
24.867	1.474177	−0.4	30.692	−0.5
29.967	1.471623	0.4	30.886	−0.3
34.896	1.469087	1.3	30.998	−0.1
40.009	1.466385	0.2	31.043	0.5
44.936	1.463716	−0.9	31.023	0.7
49.840	1.460998	−0.3	30.944	0.1
54.807	1.458181	0.3	30.809	−0.5
60.376	1.454946	−1.1	30.596	−0.2
65.051	1.452173	1.1	30.368	−0.6
70.119	1.449101	0.9	30.074	0.1
75.041	1.446053	−1.5	29.743	1.2
79.578	1.443193	0.5	29.399	−0.6
		2.4577*m*		
5.063	1.534748	−0.5	29.985	−0.3
10.001	1.532375	1.7	30.555	0.4
15.009	1.529903	−1.7	31.017	0.7
20.039	1.527363	0.4	31.378	−0.6
24.867	1.524865	−0.6	31.641	−0.4
29.967	1.522166	0.0	31.838	−0.2
34.896	1.519500	1.8	31.958	−0.3
40.009	1.516671	−0.2	32.016	0.5
44.936	1.513887	−1.4	32.012	0.8
49.840	1.511065	−0.0	31.953	0.0
54.807	1.508150	0.2	31.842	−0.4
60.376	1.504816	−0.3	31.659	−0.4
65.051	1.501964	0.9	31.459	−0.5
70.119	1.498816	0.5	31.197	0.2
75.041	1.495700	−1.4	30.901	1.0
79.578	1.492780	0.5	30.590	−0.5
		2.7232*m*		
5.063	1.584348	−0.2	30.941	−0.4
10.001	1.581806	0.5	31.485	0.6
15.009	1.579173	−0.5	31.929	0.3
20.039	1.576476	1.0	32.280	−0.7
24.867	1.573834	−1.9	32.540	−0.0
29.967	1.570996	0.3	32.738	−0.2
34.896	1.568201	0.9	32.865	0.0
40.009	1.565252	2.1	32.932	−0.1
44.936	1.562354	−1.9	32.943	0.8
49.840	1.559428	−1.4	32.901	0.4
54.807	1.556416	0.3	32.809	−0.4
60.376	1.552981	0.9	32.651	−0.7
65.051	1.550047	0.1	32.476	−0.2
70.119	1.546819	0.7	32.243	0.1
75.041	1.543631	−1.5	31.977	0.9
79.578	1.540651	0.6	31.696	−0.5
		3.0085*m*		
5.063	1.635914	0.1	31.926	−0.4
10.001	1.633199	−0.1	32.445	0.7
15.009	1.630399	−0.2	32.871	0.2
20.039	1.627543	0.6	33.212	−0.5
24.867	1.624757	−0.7	33.467	−0.3
29.967	1.621772	−0.5	33.667	−0.0
34.896	1.618846	1.3	33.798	−0.1
40.009	1.615765	0.5	33.875	0.3
44.936	1.612754	−1.1	33.896	0.6
49.840	1.609720	0.1	33.869	0.0
54.807	1.606604	−0.9	33.796	−0.1
60.376	1.603063	0.4	33.660	−0.5
65.051	1.600049	1.2	33.506	−0.5
70.119	1.596737	0.4	33.299	0.2
75.041	1.593474	−1.7	33.060	0.9
79.578	1.590430	0.7	32.806	−0.5
		3.2635*m*		
5.063	1.680454	−0.0	32.790	−0.3
10.001	1.677598	0.3	33.287	0.6
15.009	1.674661	−0.5	33.699	0.3
20.039	1.671674	0.6	34.030	−0.5
24.867	1.668770	−0.6	34.279	−0.3
29.967	1.665667	−0.4	34.477	−0.1
34.896	1.662635	1.2	34.610	−0.0
40.009	1.659451	0.9	34.691	0.2
44.936	1.656344	−2.3	34.721	0.8
49.840	1.653225	1.0	34.703	−0.2
54.807	1.650025	−0.1	34.642	−0.2
60.376	1.646396	−0.6	34.523	−0.2
65.051	1.643314	1.2	34.385	−0.4
70.119	1.639933	0.5	34.197	0.1
75.041	1.636608	−1.4	33.978	0.7
79.578	1.633511	0.6	33.744	−0.4

±0.2% in α; ±0.5% in ϕ_E, increasing at lower concentrations; and errors in $\bar{V}_2$ and $\bar{E}_2$ similar to ϕ_V and ϕ_E, but larger. In the previous paper the results of our dilatometric method compare favorably with the available data in the literature.

Due to the number of derived quantities available from the experimental densities, together with three independent variables, *T*, *m*, and ionic radius (eight salts), the number of possible graphs is large. A rather complete set of graphs, including graphs of $\bar{V}_1$ and $\bar{E}_1$, appears in the dissertation of one of the authors (A.H.) (*5*), together with calculated values of all the properties at even temperature and concentration intervals. In the following we shall present only those graphs showing typical behavior.

Selected graphs of the temperature and concentration dependence of the various properties are shown in Figures 1–6. Figure 1 shows a sample of the experimental ϕ_V data for $YbCl_3$. The distinctive behavior of $SmCl_3$ and $GdCl_3$ should be noticed in Figures 2 and 4. The downward trend in α for $YbCl_3$ at high concentrations shown in Figure 3 also occurs in $ErCl_3$ and $DyCl_3$, while α for $GdCl_3$ and $SmCl_3$ increases at high concentrations like $NdCl_3$ [shown in the previous paper (*4*)]. $\bar{E}_2$ for $GdCl_3$ shown in Figure 5 has a considerable spread with temperature at the highest concentrations while $\bar{E}_2$ for $ErCl_3$ shown in Figure 6 converges to a sharp point. With respect to this high concentration behavior in $\bar{E}_2$, $SmCl_3$ shows a spread as in $GdCl_3$, and $\bar{E}_2$ for $DyCl_3$ and $YbCl_3$ converge to a point as in $ErCl_3$. In contrast, $\bar{E}_2$ for $LaCl_3$, $PrCl_3$, and $NdCl_3$ crossed just below 3.5*m*.

Taken together with the graphs shown in the previous paper (*4*) on the light rare earths, to a certain extent the rare earths can be placed into three groups: the light rare earths (La, Pr, Nd), the intermediate rare earths (Sm, Gd), and the heavy rare earths (Dy, Er, Yb) which are similar to the light rare earths in some respects. The properties change smooth-

Table III. Density and ϕ_V for $DyCl_3$

t, °C	d, g/ml	$\Delta d \times 10^6$	ϕ_V, ml/mol	$\Delta\phi_V \times 10^3$
		0.099896m		
5.037	1.025323	−0.6	14.902	−5.2
10.011	1.024929	1.0	16.108	10.8
15.022	1.024224	0.4	16.976	0.4
20.064	1.023237	−0.6	17.581	−5.8
24.923	1.022047	−0.8	17.954	−5.5
30.040	1.020565	−0.3	18.153	−1.4
34.956	1.018938	0.1	18.183	5.8
40.086	1.017044	0.8	18.054	4.4
45.037	1.015040	1.0	17.795	−0.5
49.989	1.012871	0.5	17.418	−4.0
54.899	1.010567	−1.4	16.948	6.1
60.420	1.007807	−1.3	16.279	2.3
63.838	1.006013	0.8	15.785	−15.2
70.132	1.002539	0.6	14.803	3.3
75.447	0.999444	0.3	13.848	11.2
79.524	0.996974	−0.3	13.025	−6.6
		0.24062m		
5.037	1.060409	−0.8	16.753	−1.4
10.011	1.059844	1.5	17.880	2.8
15.022	1.058996	0.9	18.719	−1.6
20.064	1.057888	−2.4	19.326	4.7
24.923	1.056608	0.1	19.692	−5.9
30.040	1.055047	0.3	19.907	−3.0
34.956	1.053360	−0.1	19.960	3.0
40.086	1.051418	0.7	19.866	2.4
45.037	1.049379	0.8	19.651	0.6
49.989	1.047185	−0.1	19.326	0.8
54.899	1.044866	−0.6	18.900	−1.1
60.420	1.042097	−1.6	18.311	2.0
63.838	1.040303	1.1	17.877	−7.5
70.132	1.036836	0.0	16.992	3.7
75.447	1.033758	0.7	16.121	2.9
79.524	1.031305	−0.5	15.381	−2.3
		0.40211m		
5.037	1.099956	−0.2	18.417	−2.4
10.011	1.099200	0.6	19.484	3.8
15.022	1.098193	−1.0	20.282	3.4
20.064	1.096961	0.8	20.846	−4.8
24.923	1.095576	0.6	21.209	−4.9
30.040	1.093924	−2.0	21.429	3.4
34.956	1.092170	0.1	21.486	1.5
40.086	1.090172	2.1	21.411	−1.8
45.037	1.088087	−1.0	21.233	4.8
49.989	1.085863	0.4	20.939	−0.9
54.899	1.083523	−0.1	20.555	−1.9
60.420	1.080738	−2.6	20.023	3.3
63.838	1.078943	2.2	19.624	−6.8
70.132	1.075478	0.7	18.812	0.5
75.447	1.072406	−1.2	18.025	6.3
79.524	1.069968	0.4	17.349	−3.5
		0.58323m		
5.037	1.143434	−0.1	20.039	−1.7
10.011	1.142483	0.2	21.029	3.3
15.022	1.141315	0.2	21.773	0.5
20.064	1.139944	−0.2	22.308	−1.8
24.923	1.138450	−0.3	22.653	−1.9
30.040	1.136705	−0.4	22.858	−0.2
34.956	1.134876	0.4	22.921	0.5
40.086	1.132814	0.5	22.863	1.4
45.037	1.130685	0.2	22.697	1.3
49.989	1.128424	−0.2	22.433	0.4
54.899	1.126059	−0.8	22.082	−0.2
60.420	1.123260	−0.6	21.586	−1.0
63.838	1.121456	1.0	21.226	−2.8
70.132	1.117992	0.7	20.471	0.5
75.447	1.114931	−1.1	19.741	4.1
79.524	1.112505	0.4	19.116	−2.4
		0.77347m		
5.037	1.188145	−0.1	21.543	−1.4
10.011	1.187009	0.1	22.460	2.6
15.022	1.185685	0.1	23.151	0.5
20.064	1.184182	0.1	23.649	−1.7
24.923	1.182582	−0.3	23.971	−1.5
30.040	1.180746	−0.0	24.165	−0.5
34.956	1.178843	0.0	24.226	0.8
40.086	1.176720	−0.2	24.174	1.8
45.037	1.174545	0.5	24.020	0.7
49.989	1.172249	0.3	23.776	−0.2
54.899	1.169858	−0.7	23.449	−0.3
60.420	1.167042	0.1	22.986	−1.5
63.838	1.165232	0.4	22.652	−1.3
70.132	1.161768	−0.6	21.949	1.9
75.447	1.158717	0.7	21.264	1.0
79.524	1.156298	−0.3	20.687	−1.0
		0.98284m		
5.037	1.236260	−0.1	23.024	−1.1
10.011	1.234944	0.3	23.863	1.9
15.022	1.233465	−0.3	24.499	0.7
20.064	1.231831	−0.2	24.960	−1.0
24.923	1.230124	0.2	25.258	−1.6
30.040	1.228193	0.4	25.438	−0.8
34.956	1.226214	−0.4	25.496	1.0
40.086	1.224028	0.2	25.448	1.0
45.037	1.221802	−0.6	25.307	1.4
49.989	1.219469	0.8	25.079	−0.7
54.899	1.217050	−0.8	24.776	−0.2
60.420	1.214214	−0.4	24.346	−0.8
63.838	1.212397	1.0	24.035	−1.5
70.132	1.208928	−0.1	23.380	1.0
75.447	1.205880	−0.5	22.745	1.9
79.524	1.203470	0.2	22.208	−1.3
		1.2040m		
5.037	1.285873	−0.1	24.424	−0.9
10.011	1.284387	0.2	25.194	1.6
15.022	1.282761	−0.1	25.779	0.4
20.064	1.281000	−0.3	26.204	−0.8
24.923	1.279189	0.3	26.479	−1.4
30.040	1.277165	0.2	26.646	−0.5
34.956	1.275112	−0.3	26.700	0.7
40.086	1.272861	−0.0	26.656	1.0
45.037	1.270585	0.0	26.525	0.8
49.989	1.268212	0.5	26.314	−0.3
54.899	1.265763	−0.3	26.033	−0.5
60.420	1.262902	−0.5	25.634	−0.6
63.838	1.261075	0.4	25.345	−0.9
70.132	1.257598	0.4	24.736	0.5
75.447	1.254551	−0.4	24.145	1.5
79.524	1.252149	0.1	23.645	−1.0
		1.4377m		
5.037	1.337002	−0.3	25.766	−0.6
10.011	1.335358	0.7	26.470	1.1
15.022	1.333592	0.1	27.007	0.3
20.064	1.331707	−0.5	27.399	−0.6
24.923	1.329793	−0.5	27.655	−0.7
30.040	1.327677	0.5	27.810	−0.6
34.956	1.325546	−0.0	27.862	0.5
40.086	1.323227	0.2	27.823	0.8
45.037	1.320897	−0.0	27.704	0.7
49.989	1.318479	0.9	27.510	−0.5
54.899	1.315994	−0.8	27.251	−0.1
60.420	1.313103	−1.2	26.883	−0.1
63.838	1.311263	0.9	26.615	−1.0
70.132	1.307770	0.3	26.051	0.5
75.447	1.304718	−0.1	25.503	1.0
79.524	1.302316	−0.1	25.039	−0.7
		1.6713m		
5.037	1.386772	0.1	26.987	−0.7
10.011	1.384983	0.0	27.637	1.3
15.022	1.383089	−0.1	28.134	0.3
20.064	1.381092	−0.7	28.498	−0.4
24.923	1.379083	0.6	28.736	−1.1
30.040	1.376877	0.6	28.882	−0.6
34.956	1.374673	−0.2	28.932	0.5
40.086	1.372288	−0.1	28.898	0.8
45.037	1.369904	−0.6	28.790	0.9
49.989	1.367440	−0.4	28.612	0.2
54.899	1.364921	0.7	28.371	−0.8
60.420	1.361997	0.3	28.030	−0.8
63.838	1.360139	−0.1	27.783	−0.4
70.132	1.356624	0.1	27.260	0.5

Table III. Continued

t, °C	d, g/ml	Δd × 10⁶	ϕ_V, ml/mol	$\Delta\phi_V$ × 10³
		1.6713*m*		
75.447	1.353562	−0.6	26.751	1.1
79.524	1.351156	0.3	26.320	−0.8
		1.9291*m*		
5.037	1.440219	0.2	28.225	−0.6
10.011	1.438288	−0.5	28.821	1.3
15.022	1.436266	0.3	29.280	0.1
20.064	1.434153	0.0	29.617	−0.6
24.923	1.432042	0.3	29.840	−0.8
30.040	1.429742	−0.2	29.979	−0.2
34.956	1.427458	−0.4	30.028	0.5
40.086	1.425000	0.1	30.000	0.6
45.037	1.422554	0.2	29.903	0.4
49.989	1.420037	0.3	29.741	−0.1
54.899	1.417471	−0.3	29.523	−0.3
60.420	1.414504	−0.7	29.210	−0.3
63.838	1.412626	1.0	28.983	−0.7
70.132	1.409076	−0.3	28.502	0.6
75.447	1.405994	0.0	28.033	0.7
79.524	1.403575	0.0	27.636	−0.5
		2.1896*m*		
5.602	1.492445	0.5	29.441	−0.7
10.023	1.490609	−1.2	29.925	1.3
15.016	1.488476	0.3	30.348	0.2
20.057	1.486255	0.8	30.662	−0.7
24.873	1.484068	0.4	30.870	−0.7
30.041	1.481653	−0.5	31.004	−0.0
34.991	1.479273	−0.9	31.054	0.5
40.024	1.476789	−0.0	31.033	0.5
44.923	1.474307	0.7	30.948	0.1
49.944	1.471698	0.1	30.802	−0.1
54.878[a]	1.469084	14.1	30.597	−5.2
60.407	1.466051	0.1	30.316	−0.6
63.822	1.464146	−0.6	30.108	−0.2
70.160	1.460533	0.6	29.662	0.2
75.094	1.457645	−0.3	29.264	0.7
79.608	1.454946	0.1	28.860	−0.4
		2.4513*m*		
5.602	1.543611	−0.2	30.503	−0.4
10.023	1.541677	0.7	30.949	0.6
15.016	1.539435	−0.9	31.343	0.5
20.057	1.537117	0.3	31.637	−0.5
24.873	1.534843	−0.0	31.832	−0.5
30.041	1.532343	0.1	31.959	−0.2
34.991	1.529888	−0.7	32.009	0.4
40.024	1.527335	1.5	31.993	0.0
44.923	1.524789	0.1	31.918	0.3
49.944	1.522121	−1.9	31.786	0.6
54.878	1.519445	0.8	31.603	−0.5
60.407	1.516375	−0.8	31.341	−0.2
63.822	1.514445	1.4	31.149	−0.7
70.160	1.510785	0.4	30.738	0.2
75.094	1.507866	−1.2	30.370	0.9
79.608	1.505145	0.5	29.997	−0.5
		2.7203*m*		
5.602	1.594626	−0.2	31.518	−0.4
10.023	1.592605	0.2	31.931	0.7
15.016	1.590273	1.0	32.296	−0.0
20.057	1.587863	−1.1	32.570	−0.1
24.873	1.585511	0.0	32.753	−0.5
30.041	1.582931	−1.0	32.874	0.1
34.991	1.580409	2.0	32.922	−0.3
40.024	1.577785	0.0	32.910	0.4
44.923	1.575180	−2.1	32.844	0.9
49.944	1.572461	1.7	32.722	−0.4
54.878	1.569731	0.4	32.555	−0.4
60.407	1.566607	−1.7	32.315	0.0
63.822	1.564648	0.9	32.139	−0.5
70.160	1.560933	−0.8	31.761	0.5
75.094	1.557979	1.1	31.420	0.2
79.608	1.555222	−0.4	31.077	−0.2
		2.9640*m*		
5.602	1.639492	0.1	32.387	−0.4
10.023	1.637404	0.1	32.773	0.6
15.016	1.635000	−1.1	33.115	0.5
20.057	1.632527	1.2	33.371	−0.6
24.873	1.630113	0.2	33.543	−0.5
30.041	1.627472	−0.1	33.656	−0.2
34.991	1.624892	−0.7	33.703	0.4
40.024	1.622219	−0.3	33.692	0.5
44.923	1.619569	1.6	33.630	−0.1
49.944	1.616799	−1.2	33.519	0.3
54.878	1.614029	−0.2	33.363	−0.2
60.407	1.610865	0.4	33.138	−0.5
63.822	1.608879	0.2	32.974	−0.3
70.160	1.605125	0.1	32.620	0.2
75.094	1.602139	−0.5	32.302	0.6
79.608	1.599358	0.2	31.980	−0.4
		3.2868*m*		
5.602	1.696806	−0.1	33.502	−0.3
10.023	1.694655	0.5	33.854	0.5
15.016	1.692180	−1.3	34.166	0.5
20.057	1.689639	1.2	34.399	−0.6
24.873	1.687163	−0.1	34.556	−0.4
30.041	1.684460	−0.3	34.660	−0.1
34.991	1.681823	−0.2	34.701	0.2
40.024	1.679094	0.2	34.691	0.3
44.923	1.676391	−0.1	34.635	0.3
49.944	1.673574	0.3	34.531	−0.0
54.878	1.670757	−0.1	34.388	−0.2
60.407	1.667542	−0.5	34.181	−0.2
63.822	1.665527	0.3	34.030	−0.3
70.160	1.661719	0.5	33.704	0.1
75.094	1.658692	−0.6	33.413	0.5
79.608	1.655875	0.2	33.117	−0.3

[a] Entry not used in the least-squares fits.

ly from one group to the next, and membership in the three groups shifts to some extent with concentration and temperature.

Discussion

A detailed discussion of the concentration and temperature dependence of the several properties appears in the previous paper and will not be repeated here. The variation of the partial molal volumes of the solute with cationic radius (*22*) for the rare earth chloride solutions examined are shown in Figures 7–9 at several constant temperatures and concentrations. At 25°C the reversal in $\bar{V}_2$ in the middle of the rare earth series has been attributed to a shift in an equilibrium between two inner sphere water coordination numbers of the rare earth cations (*14, 15, 18*). From La to Nd the higher inner sphere water coordination is preferred. Due to the decreasing size of the rare earth ion, the equilibrium between the two coordination numbers shifts from the higher to the lower coordination between Nd and Tb. From Tb to Lu the lower inner sphere water coordination predominates. Since this is a cation effect, the position of the hydration shift in the rare earth series should be independent of the anion at infinite dilution. At infinite dilution and 25°C this two-series effect does indeed appear between Nd and Tb in the partial molal volumes of the rare earth chlorides (*14, 15, 18*), perchlorates (*14, 20*), and nitrates (*14, 15, 19*).

Similarly, to establish if the equilibrium between the two coordination numbers is shifted with a change in temperature, we must look at the lowest concentrations available, so that the cation hydration is independent of the chloride ions. That

Table IV. Density and ϕ_V for $ErCl_3$

t, °C	d, g/ml	$\Delta d \times 10^6$	ϕ_V, ml/mol	$\Delta\phi_V \times 10^3$
		0.094238*m*		
5.602	1.024496	−0.8	13.133	−4.0
10.023	1.024133	1.2	14.216	7.9
15.016	1.023432	0.5	15.123	1.1
20.057	1.022445	−0.3	15.764	−7.3
24.873	1.021266	−1.0	16.170	−3.5
30.041	1.019770	−0.8	16.406	3.0
34.991	1.018129	0.0	16.456	5.5
40.024	1.016271	1.2	16.347	−1.0
44.923	1.014287	1.1	16.116	−1.1
49.944	1.012088	0.0	15.758	1.5
54.878	1.009773	−0.4	15.285	−3.0
60.407	1.007005	−1.1	14.636	1.0
63.822	1.005210	−0.4	14.164	−3.0
70.160	1.001707	0.3	13.175	4.5
75.094	0.998835	1.4	12.283	−1.2
79.608	0.996100	−0.8	11.392	−0.4
		0.23873*m*		
5.602	1.061478	−0.5	15.079	−2.7
10.023	1.060949	0.8	16.113	4.8
15.016	1.060094	0.3	16.991	1.4
20.057	1.058980	−0.2	17.621	−3.2
24.873	1.057701	−0.7	18.025	−2.6
30.041	1.056117	−0.4	18.271	−0.4
34.991	1.054409	0.3	18.349	1.3
40.024	1.052494	0.7	18.285	1.6
44.923	1.050469	0.2	18.101	2.2
49.944	1.048238	−0.1	17.795	−0.2
54.878[a]	1.045928	26.8	17.276	−113.6
60.407	1.043120	−0.5	16.812	−3.5
63.822	1.041320	−0.4	16.398	−2.0
70.160	1.037819	0.1	15.514	3.0
75.094	1.034957	0.9	14.721	2.1
79.608	1.032236	−0.5	13.920	−1.8
		0.41670*m*		
5.602	1.106188	−0.3	16.933	−2.1
10.023	1.105468	0.3	17.898	4.0
15.016	1.104434	0.7	18.722	−0.1
20.057	1.103168	−0.8	19.324	−0.8
24.873	1.101770	−0.5	19.711	−2.2
30.041	1.100080	−0.1	19.954	−1.1
34.991	1.098290	0.8	20.039	−0.5
40.024	1.096305	−0.1	19.998	2.8
44.923	1.094227	−0.1	19.840	2.5
49.944	1.091955	−0.1	19.570	0.5
54.878	1.089588	0.2	19.205	−2.2
60.407	1.086783	−0.4	18.689	−1.6
63.822	1.084976	0.4	18.313	−2.6
70.160	1.081470	−0.8	17.514	3.8
75.094	1.078615	1.1	16.791	0.7
79.608	1.075905	−0.4	16.063	−1.2
		0.60471*m*		
5.602	1.152470	−0.3	18.607	−1.4
10.023	1.151566	0.1	19.500	3.1
15.016	1.150356	1.2	20.267	−0.7
20.057	1.148942	−0.6	20.831	−0.8
24.873	1.147425	−0.5	21.197	−1.5
30.041	1.145628	−0.9	21.430	0.5
34.991	1.143754	0.3	21.515	0.4
40.024	1.141702	1.1	21.479	0.3
44.923	1.139569	0.0	21.339	1.5
49.944	1.137254	−0.3	21.092	0.6
54.878	1.134856	0.6	20.755	−2.2
60.407	1.132030	−0.1	20.278	−1.7
63.822	1.130212	−1.4	19.933	0.9
70.160	1.126704	−0.4	19.188	1.9
75.094	1.123854	2.0	18.518	−0.8
79.608	1.121152	−0.9	17.848	−0.1
		0.81039*m*		
5.602	1.202028	−0.1	20.208	−1.3
10.023	1.200943	−0.0	21.028	2.4
15.016	1.199556	0.4	21.738	0.3
20.057	1.197992	0.1	22.260	−1.4
24.873	1.196353	−0.7	22.603	−1.0
30.041	1.194447	−0.3	22.822	−0.3
34.991	1.192485	0.3	22.905	0.3
40.024	1.190360	0.5	22.875	0.9
44.923	1.188171	−0.2	22.746	1.4
49.944	1.185811	0.2	22.519	−0.1
54.878	1.183378	−0.2	22.210	−0.7
60.407	1.180525	−0.5	21.767	−0.8
63.822	1.178700	0.3	21.445	−1.2
70.160	1.175182	−0.1	20.756	1.0
75.094	1.172332	0.3	20.137	1.3
79.608	1.169642	−0.2	19.511	−1.0
		1.3138*m*		
5.088	1.318941	1.0	23.387	−1.5
9.999	1.317326	−2.7	24.150	3.2
15.017	1.315568	1.1	24.740	−0.3
20.057	1.313687	1.2	25.177	−1.6
24.887	1.311780	−0.4	25.467	−0.8
30.029	1.309645	0.1	25.653	−0.4
34.889	1.307528	−0.2	25.727	0.6
40.068	1.305171	−0.4	25.705	1.2
44.957	1.302853	−0.8	25.599	1.2
49.947	1.300396	0.1	25.411	−0.0
54.946	1.297846	0.7	25.147	−1.1
60.437	1.294943	0.7	24.777	−1.3
63.782	1.293123	−0.1	24.512	−0.5
70.065	1.289602	−0.5	23.935	1.0
74.869	1.286823	−0.4	23.428	1.3
79.282	1.284204	0.4	22.912	−1.0
		1.5830*m*		
5.088	1.378802	0.7	24.893	−1.1
9.999	1.377004	−1.7	25.585	2.1
15.017	1.375079	0.5	26.124	0.1
20.057	1.373050	0.2	26.525	−0.8
24.887	1.371022	1.6	26.790	−1.6
30.029	1.368769	−1.0	26.964	0.2
34.889	1.366560	0.1	27.033	0.3
40.068	1.364117	−0.5	27.016	1.0
44.957	1.361730	−0.6	26.920	0.9
49.947	1.359215	−0.1	26.749	0.1
54.946	1.356618	0.6	26.508	−0.8
60.437	1.353675	1.5	26.167	−1.4
63.782	1.351835	−0.9	25.925	0.0
70.065	1.348290	−0.8	25.394	0.9
74.869	1.345500	0.2	24.927	0.8
79.282	1.342876	0.2	24.453	−0.7
		1.8457*m*		
5.088	1.435473	0.7	26.241	−0.9
9.999	1.433515	−1.3	26.875	1.7
15.017	1.431442	−0.6	27.372	0.5
20.057	1.429285	1.8	27.740	−1.4
24.887	1.427143	0.1	27.988	−0.8
30.029	1.424787	−0.2	28.150	−0.2
34.889	1.422489	−0.3	28.216	0.5
40.068	1.419965	−0.7	28.203	0.9
44.957	1.417513	0.4	28.117	0.3
49.947	1.414938	−1.2	27.961	0.5
54.946	1.412293	1.5	27.740	−1.1
60.437	1.409305	0.4	27.428	−0.7
63.782	1.407444	−0.5	27.204	−0.2
70.065	1.403867	0.2	26.715	0.4
74.869	1.401058	−0.7	26.285	1.1
79.282	1.398422	0.4	25.847	−0.7
		2.1014*m*		
5.088	1.489047	0.9	27.455	−0.8
9.999	1.486953	−2.4	28.040	1.8
15.017	1.484754	1.1	28.499	−0.2
20.057	1.482477	1.3	28.843	−1.0
24.887	1.480232	−0.7	29.075	−0.4
30.029	1.477779	0.2	29.228	−0.3
34.889	1.475398	−0.4	29.293	0.4
40.068	1.472796	−0.6	29.284	0.8
44.957	1.470278	−0.0	29.207	0.5
49.947	1.467648	0.6	29.065	−0.2
54.946	1.464950	0.1	28.863	−0.4
60.437	1.461916	0.3	28.575	−0.6
63.782	1.460030	−0.3	28.368	−0.2
70.065	1.456414	−0.0	27.917	0.4

Table IV. Continued

t, °C	d, g/ml	$\Delta d \times 10^6$	ϕ_V, ml/mol	$\Delta\phi_V \times 10^3$
		2.1014m		
74.869	1.453583	−0.2	27.519	0.7
79.282	1.450931	0.2	27.113	−0.5
		2.3872m		
5.088	1.547124	0.5	28.711	−0.6
9.999	1.544896	−0.9	29.247	1.1
15.017	1.542567	−0.0	29.671	0.2
20.057	1.540173	0.3	29.989	−0.6
24.887	1.537828	0.5	30.204	−0.7
30.029	1.535274	0.2	30.348	−0.2
34.889	1.532809	0.2	30.410	0.2
40.068	1.530124	−0.2	30.404	0.6
44.957	1.527535	−2.1	30.337	1.0
49.947	1.524845	1.4	30.207	−0.4
54.946	1.522090	0.1	30.023	−0.4
60.437	1.519004	1.1	29.760	−0.8
63.782	1.517089	−0.2	29.571	−0.2
70.065	1.513424	−1.2	29.157	0.7
74.869	1.510564	0.5	28.790	0.4
79.282	1.507887	0.1	28.418	−0.4
		2.6661m		
5.088	1.602011	0.9	29.843	−0.6
9.999	1.599674	−2.4	30.336	1.4
15.017	1.597244	0.9	30.727	−0.1
20.057	1.594755	1.6	31.021	−0.8
24.887	1.592321	−0.3	31.221	−0.4
30.029	1.589683	−1.1	31.355	0.1
34.889	1.587147	0.5	31.413	0.1
40.068	1.584392	0.2	31.409	0.4
44.957	1.581744	−0.8	31.347	0.6
49.947	1.578994	−0.1	31.229	0.0
54.946	1.576190	0.3	31.060	−0.4
60.437	1.573053	1.0	30.817	−0.7
63.782	1.571110	−0.2	30.642	−0.2
70.065	1.567398	−0.8	30.260	0.6
74.869	1.564504	0.1	29.921	0.5
79.282	1.561799	0.1	29.577	−0.4
		3.0217m		
5.088	1.669536	0.8	31.169	−0.5
9.999	1.667098	−1.5	31.612	1.0
15.017	1.664568	−0.7	31.963	0.3
20.057	1.661989	2.6	32.227	−1.0
24.887	1.659470	−0.9	32.407	−0.2
30.029	1.656751	0.1	32.527	−0.2
34.889	1.654140	0.1	32.579	0.2
40.068	1.651315	−0.0	32.574	0.4
44.957	1.648605	−0.6	32.516	0.5
49.947	1.645796	−1.1	32.407	0.3
54.946	1.642941	1.1	32.251	−0.5
60.437	1.639750	0.8	32.029	−0.5
63.782	1.637778	0.3	31.869	−0.3
70.065	1.634014	−0.3	31.519	0.4
74.869	1.631081	−1.0	31.210	0.7
79.282	1.628344	0.6	30.896	−0.5
		3.3085m		
5.088	1.721988	0.7	32.166	−0.5
9.999	1.719497	−1.6	32.571	0.9
15.017	1.716919	0.6	32.892	0.0
20.057	1.714288	0.2	33.133	−0.4
24.887	1.711731	0.1	33.295	−0.4
30.029	1.708970	0.6	33.402	−0.3
34.889	1.706321	0.7	33.446	0.1
40.068	1.703457	−0.2	33.438	0.4
44.957	1.700711	−2.9	33.381	0.9
49.947	1.697873	0.6	33.277	−0.1
54.946	1.694985	1.4	33.129	−0.5
60.437	1.691759	−0.0	32.920	−0.3
63.782	1.689768	0.9	32.769	−0.4
70.065	1.685965	−0.5	32.442	0.4
74.869	1.683002	−1.1	32.153	0.7
79.282	1.680238	0.7	31.860	−0.4
		3.5697m		
5.088	1.768127	0.2	33.050	−0.4
9.999	1.765614	−0.5	33.423	0.7
15.017	1.763009	−0.1	33.717	0.1
20.057	1.760356	0.3	33.936	−0.4
24.887	1.757777	−0.2	34.083	−0.3
30.029	1.754995	0.4	34.178	−0.2
34.889	1.752328	0.4	34.215	0.1
40.068	1.749444	−0.1	34.202	0.4
44.957	1.746682	−1.0	34.144	0.5
49.947	1.743823	−0.5	34.042	0.1
54.946	1.740916	0.8	33.900	−0.4
60.437	1.737669	0.9	33.700	−0.5
63.782	1.735662	−0.1	33.557	−0.2
70.065	1.731830	−0.6	33.247	0.4
74.869	1.728844	−0.1	32.975	0.4
79.282	1.726053	0.2	32.699	−0.3

[a] Entry not used in the least-squares fits.

is, in sufficiently dilute solutions the environment beyond the inner hydration sphere consists only of water molecules and is free from complicating anion–cation interactions which may change differently across the rare earth series, giving rise to apparent shifts in the hydration change. The lowest concentration where experimental data were determined in this study was 0.1m, shown in Figure 7. From Figure 7, the change in coordination occurs in the same position in the rare earth series over the whole temperature range. Therefore, in the absence of close-range rare earth–chloride interactions, i.e., at concentrations where a large excess of water is available, the equilibrium between the two inner sphere water coordination numbers of the cation is relatively insensitive to temperature changes.

At higher concentrations the position and shape of the break in the series are strongly dependent on both the concentration and temperature as shown in Figures 8 and 9. Thus, at 2m the two-series effect occurs between Sm and Dy at 5°C and between Nd and Gd at 80°C; at 3.5m the position is between Nd and Tb at 5°C and becomes merely a change in slope near Sm at 80°C. The position of the reversal in $\bar{V}_2$ in the rare earth series at higher concentrations does not uniquely determine the position of the hydration change in the rare earth series (*20*). For example, the two-series effect in the partial molal volumes of the rare earth perchlorates at 25°C shifts from Nd–Tb at infinite dilution to the area of Tb–Dy–Ho at 3.5m (*20*), whereas the two-series effect in the conductances of the rare earth perchlorates appears between Nd and Tb at high concentrations (*16*).

It appears that as anions begin to interact with the hydrated rare earth ion at increasing concentrations, forming outer sphere complexes (in the case of the chlorides and perchlorates), the interpretation of the two-series effect will have to include changes in anion–cation interactions across the rare earth series. So far, this has only been successful with the rare earth nitrates, where the complete disappearance of the two-series effect with increasing concentration is associated with the displacement of inner sphere water dipoles by nitrate ions (*12, 19, 21*).

A distinction is being made between the "two-series effect" and the "hydration change". In sufficiently dilute solutions where the cation–water complex is essentially indepen-

Table V. Density and ϕ_V for $YbCl_3$

t, °C	d, g/ml	$\Delta d \times 10^6$	ϕ_V, ml/mol	$\Delta\phi_V \times 10^3$
		0.096912*m*		
5.073	1.025992	−0.9	10.820	−1.7
10.018	1.025597	2.2	12.073	−1.0
15.030	1.024884	−0.6	13.034	10.4
20.067	1.023891	−1.0	13.702	−2.0
24.896	1.022705	−0.4	14.124	−9.9
30.011	1.021217	−0.2	14.385	−2.7
34.910	1.019591	0.4	14.463	2.2
40.072	1.017680	1.0	14.381	1.9
44.979	1.015687	−0.1	14.175	10.6
49.920	1.013519	0.2	13.826	−0.6
54.920	1.011169	−0.1	13.359	−7.5
60.458	1.008391	−1.3	12.730	2.3
63.783	1.006640	−0.1	12.275	−6.8
70.104	1.003144	0.9	11.308	−0.5
75.008	1.000287	0.3	10.459	11.2
79.400	0.997625	−0.4	9.598	−5.9
		0.24755*m*		
5.073	1.065750	0.1	12.904	−5.1
10.018	1.065150	−0.3	14.118	10.6
15.030[a]	1.064288	14.6	14.966	−52.7
20.067	1.063144	0.5	15.671	−5.6
24.896	1.061846	−0.1	16.098	−4.6
30.011	1.060263	−0.2	16.366	−1.1
34.910	1.058561	−0.3	16.468	3.5
40.072	1.056585	0.4	16.425	3.1
44.979	1.054542	−0.1	16.260	3.9
49.920	1.052335	−0.1	15.977	0.7
54.920	1.049956	0.2	15.580	−3.8
60.458	1.047157	0.1	15.023	−4.7
63.783	1.045398	−0.2	14.632	−2.0
70.104	1.041896	−0.1	13.774	3.7
75.008	1.039044	0.2	13.006	4.8
79.400	1.036391	−0.1	12.242	−3.6
		0.42932*m*		
5.073	1.112845	−0.2	14.853	−2.2
10.018	1.112021	0.4	15.973	3.9
15.030	1.110953	0.0	16.825	1.0
20.067	1.109661	−0.8	17.446	−1.0
24.896	1.108234	−0.8	17.856	−1.5
30.011	1.106540	3.0	18.112	−7.6
34.910	1.104742	−1.7	18.231	5.0
40.072	1.102687	−0.4	18.206	3.8
44.979	1.100584	0.2	18.066	1.8
49.920	1.098328	−0.0	17.819	0.2
54.920	1.095910	0.2	17.468	−2.3
60.458	1.093081	0.2	16.968	−3.0
63.783	1.091309	0.1	16.615	−1.8
70.104	1.087793	−0.6	15.840	3.3
75.008	1.084940	0.4	15.142	2.5
79.400	1.082292	−0.1	14.451	−2.1
		0.63692*m*		
5.073	1.165535	−0.8	16.716	−0.6
10.018	1.164477	1.4	17.743	1.5
15.030	1.163205	0.7	18.532	−0.2
20.067	1.161741	−1.0	19.112	−0.5
24.896	1.160177	−0.2	19.495	−1.8
30.011	1.158355	−1.5	19.746	1.3
34.910	1.156462	−2.2	19.853	4.0
40.072	1.154328	6.3	19.826	−6.8
44.979	1.152152	−0.1	19.711	1.6
49.920	1.149839	−2.1	19.492	3.1
54.920	1.147379	−0.6	19.171	−0.5
60.458	1.144514	−1.4	18.716	0.2
63.783	1.142729	1.0	18.390	−2.6
70.104	1.139197	1.1	17.679	−0.2
75.008	1.136337	−0.3	17.043	2.6
79.400	1.133692	−0.2	16.408	−1.2
		0.85624*m*		
5.073	1.219995	0.1	18.405	−1.4
10.018	1.218713	−0.0	19.345	2.5
15.030	1.217248	−0.1	20.070	0.7
20.067	1.215617	−0.2	20.606	−1.2
24.896	1.213915	0.2	20.964	−1.8
30.011	1.211969	0.4	21.199	−0.9
34.910	1.209975	−0.3	21.303	1.1
40.072	1.207744	0.1	21.293	1.4
44.979	1.205503	−0.2	21.184	1.3
49.920	1.203135	−0.4	20.982	0.5
54.920	1.200629	0.5	20.690	−1.5
60.458	1.197726	0.0	20.272	−1.3
63.783	1.195922	−0.1	19.975	−0.7
70.104	1.192368	0.4	19.319	0.7
75.008	1.189502	−0.6	18.731	2.3
79.400	1.186858	0.2	18.145	−1.4
		1.1438*m*		
5.087	1.289572	0.2	20.337	−1.1
10.045	1.288025	−0.6	21.178	2.3
15.040	1.286338	0.7	21.826	−0.1
20.069	1.284512	−0.4	22.310	−0.8
24.890	1.282648	0.3	22.634	−1.4
29.997	1.280556	0.0	22.850	−0.4
34.896	1.278440	−0.3	22.945	0.8
40.011	1.276121	−0.3	22.941	1.3
44.947	1.273782	0.3	22.843	0.6
49.915	1.271328	0.4	22.661	−0.2
54.883	1.268778	−0.0	22.400	−0.7
60.312	1.265885	−1.1	22.030	−0.2
63.766	1.263991	1.2	21.749	−1.5
70.091	1.260405	−0.6	21.154	1.2
74.943	1.257560	0.4	20.624	1.0
79.429	1.254855	−0.1	20.082	−0.8
		1.4468*m*		
5.087	1.360652	0.0	22.137	−0.8
10.045	1.358871	0.2	22.888	1.4
15.040	1.356972	−0.3	23.471	0.5
20.069	1.354960	−0.6	23.908	−0.5
24.890	1.352939	0.7	24.202	−1.3
29.997	1.350702	1.3	24.399	−1.0
34.896	1.348463	−0.7	24.489	0.8
40.011	1.346034	−2.1	24.488	2.0
44.947	1.343608	0.7	24.400	0.3
49.915	1.341079	0.3	24.236	−0.1
54.883	1.338470	1.9	23.999	−1.6
60.312	1.335522	−1.2	23.665	−0.1
63.766	1.333599	−0.3	23.410	−0.3
70.091	1.329978	−1.0	22.869	1.2
74.943	1.327116	1.7	22.387	0.0
79.429	1.324399	−0.6	21.895	−0.3
		1.7552*m*		
5.087	1.430622	0.8	23.798	−0.9
10.045	1.428626	−2.2	24.475	2.1
15.040	1.426539	2.0	25.002	−0.5
20.069	1.424351	−0.6	25.400	−0.4
24.890	1.422182	0.7	25.670	−1.1
29.997	1.419803	−1.1	25.854	0.2
34.896	1.417450	0.7	25.937	0.1
40.011	1.414914	0.6	25.939	0.4
44.947	1.412393	−0.1	25.865	0.6
49.915	1.409783	−1.3	25.720	0.6
54.883	1.407103	−0.6	25.509	−0.2
60.312	1.404095	0.2	25.207	−0.7
63.766	1.402138	1.8	24.977	−1.2
70.091	1.398463	0.9	24.488	0.1
74.943	1.395565	−2.9	24.055	2.1
79.429	1.392834	1.2	23.606	−1.1
		2.0830*m*		
5.087	1.502408	0.4	25.424	−0.7
10.045	1.500216	−0.9	26.035	1.3
15.040	1.497945	−0.1	26.513	0.3
20.069	1.495594	0.9	26.875	−0.9
24.890	1.493278	0.5	27.124	−0.8
29.997	1.490760	−0.4	27.295	−0.1
34.896	1.488283	−0.8	27.376	0.6
40.011	1.485633	−0.3	27.383	0.7
44.947	1.483016	0.5	27.321	0.3
49.915	1.480320	0.3	27.193	−0.1
54.883	1.477563	0.1	27.006	−0.4
60.312	1.474480	−0.8	26.736	−0.3
63.766	1.472484	1.0	26.530	−0.7
70.091	1.468746	−1.0	26.090	0.8
74.943	1.465813	0.6	25.697	0.5
79.429	1.463045	−0.1	25.294	−0.4

Table V. Continued

t, °C	d, g/ml	$\Delta d \times 10^6$	ϕ_V, ml/mol	$\Delta\phi_V \times 10^3$
		2.4142*m*		
5.087	1.572262	0.2	26.938	−0.5
10.045	1.569900	−0.8	27.491	1.1
15.040	1.567472	0.8	27.926	−0.0
20.069	1.564972	0.6	28.258	−0.6
24.890	1.562526	0.1	28.487	−0.6
29.997	1.559880	−1.9	28.646	0.4
34.896	1.557295	0.8	28.723	0.0
40.011	1.554538	0.2	28.734	0.5
44.947	1.551827	0.5	28.680	0.3
49.915	1.549045	0.0	28.569	0.0
54.883	1.546211	0.2	28.402	−0.4
60.312	1.543052	−1.0	28.160	−0.2
63.766	1.541010	0.5	27.976	−0.4
70.091	1.537200	−0.7	27.579	0.6
74.943	1.534217	1.2	27.224	0.2
79.429	1.531407	−0.5	26.860	−0.3
		2.7644*m*		
5.087	1.643318	0.2	28.403	−0.4
10.045	1.640814	−1.0	28.902	1.0
15.040	1.638251	1.4	29.296	−0.2
20.069	1.635622	0.2	29.597	−0.5
24.890	1.633059	−0.7	29.806	−0.3
29.997	1.630300	−1.0	29.952	0.1
34.896	1.627612	0.4	30.024	0.1
40.011	1.624758	0.9	30.036	0.2
44.947	1.621957	−0.5	29.990	0.5
49.915	1.619095	0.3	29.890	−0.0
54.883	1.616186	0.1	29.740	−0.3
60.312	1.612952	0.0	29.523	−0.4
63.766	1.610864	−0.3	29.356	−0.2
70.091	1.606977	−1.1	28.998	0.6
74.943	1.603940	1.8	28.678	0.1
79.429	1.601079	−0.7	28.350	−0.2
		3.1214*m*		
5.087	1.712958	−0.4	29.763	−0.0
10.045	1.710348	−6.9	30.212	2.5
15.040	1.707692	1.8	30.564	0.2
20.069	1.704967	−0.8	30.836	−0.0
24.890	1.702317	−1.2	31.024	−0.2
29.997	1.699472	−0.8	31.154	−0.1
34.896	1.696705	0.8	31.218	−0.1
40.011	1.693772	0.0	31.228	0.3
44.947	1.690903	0.9	31.184	0.1
49.915	1.687973	1.1	31.093	−0.2
54.883	1.684999	−0.7	30.956	−0.0
60.312	1.681698	−2.1	30.758	0.2
63.766	1.679571	0.7	30.606	−0.4
70.091	1.675609	−0.4	30.281	0.3
74.943	1.672513	1.8	29.990	−0.0
79.429	1.669596	−0.9	29.693	−0.0
		3.4947*m*		
5.087	1.782820	0.2	31.071	−0.4
10.045	1.780152	−0.5	31.471	0.7
15.040	1.777429	0.3	31.785	0.1
20.069	1.774650	−0.2	32.024	−0.3
24.890	1.771951	−0.2	32.189	−0.4
29.997	1.769056	1.6	32.301	−0.4
34.896	1.766237	−1.2	32.354	0.4
40.011	1.763255	−1.2	32.357	0.6
44.947	1.760341	0.8	32.313	0.1
49.915	1.757362	0.5	32.226	−0.1
54.883	1.754340	0.4	32.098	−0.3
60.312	1.750983	−0.8	31.915	−0.2
63.766	1.748818	0.6	31.775	−0.3
70.091	1.744783	−1.0	31.479	0.4
74.943	1.741625	1.0	31.215	0.2
79.429	1.738648	−0.3	30.947	−0.2

[a] Entry not used in the least-squares fits.

dent of the anions and the outer spheres are made up of water molecules only, the two are directly related. However, at higher concentrations this is not necessarily so, since the break in the series is the result of not only the inner sphere hydration change, but also possible changes in the outer spheres which contain anions at higher concentrations. Therefore, without other thermodynamic, spectroscopic, and stability constant data at higher temperatures and concentrations, speculation on the significance of the changes in the position and shape of the two-series effect in $\bar{V}_2$ with temperature at higher concentrations, appearing in Figures 8 and 9, is premature.

Series plots of ϕ_V are quite similar to those for $\bar{V}_2$ and are not shown here. The ϕ_V series plots have less scatter, and the changes in the shape of the two-series effect with temperature and concentration are less pronounced than in $\bar{V}_2$—both differences being due to the integral nature of the apparent molal volume.

The variation of the coefficients of thermal expansion and the apparent molal expansibility of the rare earth chloride solutions as a function of ionic radii are shown in Figures 10–12 at several constant concentrations and temperatures. Clearly, the thermal variation of the volume properties also shows the familiar two-series effect. Considering the lowest concentration at 25°C in Figure 11, the two-series effect in ϕ_E occurs between Nd and Tb (at least somewhere between Gd and Dy), which is the same position as in other thermodynamic properties under these conditions. According to our model, La through Nd have a trend in thermal expansion displaced from the trend in Tb through Lu, whereas Sm and Gd are intermediate. In our view these arise from the difference in the total hydration between the light and heavy rare earth cations as determined by the change in the inner sphere water coordination. Again, for dilute solutions, the position of the two-series effect in ϕ_E across the series changes very little with temperature, whereas at higher concentrations this is not the case. Series graphs of E_2 and E_1 give information similar to that of ϕ_E and have been omitted.

The $\bar{V}_2^0$ and $\bar{E}_2^0$ obtained from the extrapolation to infinite dilution with the Redlich-Meyer equation are shown in Figures 13–15. The $\bar{V}_2^0$ obtained from magnetic float measurements (*14*) at 25°C are also included in Figure 13. The maxima, T_{max}, in $\bar{V}_2^0$ vs. t, Figure 15, are listed in Table X. The values at infinite dilution obtained from this extrapolation should be considered tentative until measurements in the dilute ($<0.1m$) region are obtained. Although the agreement in the case of $\bar{V}_2^0$ is good at 25°C, $\bar{V}_2^0$ at other temperatures and the $\bar{E}_2^0$ values may be slightly in error. However, the trends in $\bar{V}_2^0$ and $\bar{E}_2^0$ across the series show very little scatter as seen in Figures 13 and 14 and should be at least self-consistent. They are, in fact, very close to the trends in the most dilute experimental region.

Intuitive, empirical, and semitheoretical considerations (*9*) indicate that the amount of electrostriction of the solvent by a cation through ion–water dipole interactions should increase with the surface charge density of the cation, resulting in a decrease in the cationic partial molal volume, $\bar{V}^0$ (ion), with increasing charge, Z, and decreasing radius, r. This has been generally found to be true for monovalent and divalent cations (*9*), although the exact functional dependence is not certain [i.e., whether the electrostriction is proportional to Z^2/r, $Z^{3/2}/r$, Z/r, Z/r^2, or more complex functions (*9*)]. The $\bar{V}^0$ (ion) for the trivalent rare earth ions (*14*) fit these trends in

Table VI. Density Parameters Corresponding to Equation 1

Molality	C_0	$C_1 \times 10^4$	$C_2 \times 10^6$	$C_3 \times 10^8$	$C_4 \times 10^{10}$	$C_5 \times 10^{13}$
			$SmCl_3$			
0.098490	1.0240228	0.24854	−7.68989	5.96896	−3.92697	11.9601
0.23601	1.0571897	−0.25672	−6.74274	4.81466	−3.01014	8.7839
0.40942	1.0982510	−0.85962	−5.65644	3.53718	−2.06200	5.7467
0.59909	1.1422273	−1.42907	−4.83414	2.82541	−1.65501	4.6434
0.79726	1.1872190	−1.99299	−3.98285	1.93103	−1.00406	2.4631
1.0194	1.2365241	−2.56169	−3.23026	1.25813	−0.57537	1.1614
1.2623	1.2891130	−3.11784	−2.60478	0.79467	−0.33390	0.5363
1.5089	1.3410969	−3.64377	−2.03768	0.25394	0.11519	−1.3160
1.7430	1.3891321	−4.09996	−1.65163	0.04688	0.13804	−0.9767
2.0041	1.4412045	−4.55664	−1.38928	−0.05627	0.19080	−1.1870
2.2697	1.4925706	−5.00238	−1.15096	−0.16384	0.23170	−1.1457
2.5663	1.5479881	−5.42482	−1.20810	0.36374	−0.37027	1.4014
2.8531	1.5997271	−5.85487	−0.95247	−0.14653	0.36766	−2.1856
3.1436	1.6502118	−6.23030	−0.98448	0.15172	0.08467	−1.0045
3.4579	1.7026641	−6.61429	−1.02955	0.56690	−0.35712	0.8206
			$GdCl_3$			
0.097765	1.0242562	0.27581	−7.67345	5.88416	−3.83192	11.6301
0.23685	1.0583521	−0.17609	−6.80601	4.85869	−3.04458	8.9523
0.41052	1.1001593	−0.71574	−5.77769	3.61810	−2.07531	5.6368
0.58944	1.1423465	−1.19739	−4.99603	2.86264	−1.58393	4.1682
0.78425	1.1873506	−1.69648	−4.15134	1.91688	−0.87408	1.8198
0.99472	1.2348807	−2.14743	−3.56509	1.51786	−0.71424	1.5841
1.2239	1.2854285	−2.59982	−3.03827	1.25788	−0.73841	2.2978
1.4444	1.3329257	−3.01576	−2.50005	0.69779	−0.25695	0.3952
1.7108	1.3888210	−3.46406	−2.09921	0.52786	−0.23340	0.4566
1.9407	1.4357741	−3.83147	−1.80376	0.37939	−0.16561	0.2750
2.1911	1.4855883	−4.23227	−1.44470	0.00487	0.20222	−1.2648
2.4577	1.5371221	−4.62902	−1.17072	−0.25462	0.53223	−2.9577
2.7232	1.5868985	−4.98074	−1.13115	0.15347	−0.01625	−0.4957
3.0085	1.6386504	−5.35660	−0.95347	0.09950	0.07681	−1.1485
3.2635	1.6833407	−5.65782	−0.87533	0.32599	−0.26024	0.4298
			$DyCl_3$			
0.099896	1.0253787	0.26149	−7.66234	5.91314	−3.87981	11.7989
0.24062	1.0606748	−0.19281	−6.86027	5.15807	−3.47715	11.0518
0.40211	1.1004553	−0.70571	−5.85000	3.85960	−2.38026	7.0087
0.58323	1.1441678	−1.21389	−4.96381	2.92299	−1.72754	5.0002
0.77347	1.1891027	−1.69797	−4.11867	1.97087	−0.97160	2.2603
0.98284	1.2374297	−2.15367	−3.41715	1.31941	−0.52613	0.7723
1.2040	1.2872424	−2.57859	−2.81479	0.86148	−0.31678	0.4632
1.4377	1.3385536	−2.96426	−2.33279	0.53506	−0.15959	0.1125
1.6713	1.3884878	−3.31075	−1.92136	0.25705	−0.01238	−0.3008
1.9291	1.4420946	−3.64365	−1.58443	0.05950	0.10295	−0.7388
2.1896	1.4946976	−3.95008	−1.25797	−0.26492	0.42557	−2.2076
2.4513	1.5460003	−4.20421	−1.06917	−0.35838	0.50402	−2.5880
2.7203	1.5971281	−4.40819	−1.03005	−0.14897	0.24619	−1.6341
2.9640	1.6420849	−4.57867	−0.88230	−0.34790	0.48551	−2.7527
3.2868	1.6994821	−4.72764	−0.86875	−0.20713	0.31100	−2.0953
			$ErCl_3$			
0.094238	1.0245764	0.27191	−7.70204	5.97153	−3.93126	11.9876
0.23873	1.0618114	−0.23197	−6.72747	4.78482	−3.00674	8.8917
0.41670	1.1068112	−0.80489	−5.67798	3.56789	−2.09156	5.8979
0.60471	1.1533716	−1.35090	−4.73071	2.51385	−1.28237	3.0760
0.81039	1.2031967	−1.87119	−3.94204	1.83671	−0.90719	2.1917
1.3138	1.3204881	−2.91823	−2.47397	0.59922	−0.14217	−0.0696
1.5830	1.3805649	−3.36977	−1.91747	0.15413	0.18313	−1.3164
1.8457	1.4374224	−3.75810	−1.46964	−0.20668	0.45939	−2.4032
2.1014	1.4911456	−4.05850	−1.33527	0.09718	−0.01847	−0.1790
2.3872	1.5493774	−4.37549	−1.05064	−0.10058	0.15857	−1.0279
2.6661	1.6043812	−4.61147	−0.94555	0.02354	−0.02145	−0.3537
3.0217	1.6720159	−4.83374	−0.83599	0.01495	0.03593	−0.9944
3.3085	1.7245288	−4.95783	−0.71774	−0.12614	0.16885	−1.6342
3.5697	1.7706928	−5.00444	−0.75776	0.09325	−0.14445	−0.3029
			$YbCl_3$			
0.096912	1.0260520	0.25926	−7.71261	6.02405	−3.99467	12.2341
0.24755	1.0660610	−0.28928	−6.61153	4.54605	−2.73796	7.7158
0.42932	1.1134305	−0.87977	−5.58682	3.40989	−1.91207	5.0667
0.63692	1.1664078	−1.49383	−4.56997	2.36285	−1.21628	3.0516
0.85624	1.2211309	−2.05211	−3.77041	1.67251	−0.79234	1.8004
1.1438	1.2910202	−2.70576	−2.81965	0.73423	−0.08409	−0.7245
1.4468	1.3623716	−3.26882	−2.19357	0.40104	0.03415	−0.9960
1.7552	1.4325817	−3.76621	−1.72065	0.28620	−0.11715	0.1680
2.0830	1.5045897	−4.22433	−1.28050	−0.08078	0.25107	−1.6045
2.4142	1.5746309	−4.60455	−1.02931	−0.06736	0.12191	−0.9607
2.7644	1.6458406	−4.91348	−0.88900	−0.01420	0.07629	−1.1323
3.1214	1.7155849	−5.11875	−0.89764	0.24791	−0.19498	−0.4213
3.4947	1.7855207	−5.27411	−0.69159	−0.11424	0.15676	−2.1156

Table VII. Apparent Molal Volume Parameters Corresponding to Equation 3

Molality	A_0	$A_1 \times 10^1$	$A_2 \times 10^3$	$A_3 \times 10^5$	$A_4 \times 10^7$	$A_5 \times 10^9$
			$SmCl_3$			
0.098490	11.3569	3.76407	−8.86104	10.17113	−8.02041	2.66555
0.23601	13.1397	3.62880	−8.40188	9.66639	−7.66363	2.58796
0.40942	14.9627	3.41895	−7.78033	8.82764	−6.84779	2.26386
0.59909	16.7122	3.13051	−6.80654	7.26900	−5.42547	1.75304
0.79726	18.2901	2.90356	−6.18864	6.51952	−4.85449	1.57478
1.0194	19.8546	2.67339	−5.54825	5.68829	−4.17962	1.34626
1.2623	21.3843	2.45216	−4.93435	4.90321	−3.54247	1.12979
1.5089	22.7872	2.26798	−4.45211	4.38684	−3.20492	1.04393
1.7430	24.0215	2.11512	−4.03611	3.87988	−2.77723	0.88455
2.0041	25.3119	1.96286	−3.61593	3.40846	−2.43402	0.77614
2.2697	26.5435	1.83499	−3.27193	3.03701	−2.15703	0.68098
2.5663	27.8464	1.70132	−2.88043	2.53888	−1.74258	0.53184
2.8531	29.0341	1.60343	−2.65499	2.41030	−1.75181	0.56727
3.1436	30.1848	1.50951	−2.40296	2.12271	−1.52896	0.48855
3.4579	31.3914	1.42218	−2.17572	1.84966	−1.30464	0.40771
			$GdCl_3$			
0.097765	13.9868	3.51653	−9.06914	10.98435	−8.88331	2.93747
0.23685	15.8173	3.29196	−8.12801	9.41187	−7.43935	2.48082
0.41052	17.5703	3.08718	−7.50011	8.59769	−6.77046	2.26778
0.58944	19.1685	2.83627	−6.67542	7.30946	−5.59888	1.84269
0.78425	20.6740	2.63129	−6.11098	6.62529	−5.05795	1.66146
0.99472	22.1418	2.40138	−5.41103	5.59975	−4.15273	1.33666
1.2239	23.5505	2.19960	−4.81058	4.74231	−3.37383	1.04158
1.4444	24.7675	2.04565	−4.40763	4.33456	−3.13380	0.99005
1.7108	26.1010	1.88030	−3.92654	3.73792	−2.66124	0.83430
1.9407	27.1536	1.76248	−3.58848	3.35240	−2.37480	0.74301
2.1911	28.2125	1.65970	−3.30649	3.09247	−2.22650	0.70895
2.4577	29.2687	1.56241	−3.03216	2.83063	−2.08185	0.68136
2.7232	30.2638	1.47209	−2.74836	2.44606	−1.73572	0.55026
3.0085	31.2839	1.39211	−2.52944	2.22584	−1.59417	0.51349
3.2635	32.1770	1.32536	−2.34767	2.00313	−1.39937	0.44024
			$DyCl_3$			
0.099896	13.3181	3.58726	−9.08701	10.60557	−8.39091	2.79019
0.24062	15.2791	3.30459	−7.84527	8.13059	−5.65916	1.62940
0.40211	17.0236	3.12845	−7.50417	8.24309	−6.23910	2.01347
0.58323	18.7494	2.88816	−6.81025	7.30436	−5.45041	1.73994
0.77347	20.3521	2.66624	−6.24262	6.66438	−5.03218	1.64166
0.98284	21.9353	2.43151	−5.61105	5.84164	−4.37534	1.42837
1.2040	23.4294	2.21882	−5.04614	5.08853	−3.72093	1.18657
1.4377	24.8576	2.02081	−4.52710	4.44307	−3.20680	1.01314
1.6713	26.1530	1.85510	−4.10535	3.94803	−2.82814	0.89072
1.9291	27.4604	1.69625	−3.70158	3.49293	−2.49467	0.78822
2.1896	28.6683	1.56044	−3.36960	3.16048	−2.28210	0.73353
2.4513	29.7890	1.43790	−3.06566	2.83172	−2.04015	0.65599
2.7203	30.8599	1.32279	−2.77662	2.49481	−1.77082	0.56584
2.9640	31.7733	1.23402	−2.58543	2.33375	−1.67973	0.54454
3.2868	32.9434	1.12258	−2.33761	2.07381	−1.47794	0.47686
			$ErCl_3$			
0.094238	11.3600	3.63859	−8.85726	9.75309	−7.30628	2.29498
0.23873	13.3857	3.46963	−8.39915	9.54426	−7.41859	2.43572
0.41670	15.3598	3.21323	−7.61831	8.45484	−6.45909	2.09289
0.60471	17.1538	2.96036	−6.91332	7.54640	−5.77522	1.89633
0.81039	18.8808	2.69683	−6.15077	6.42380	−4.76453	1.52299
1.3138	22.3906	2.19699	−4.85996	4.82648	−3.52079	1.12072
1.5830	23.9903	1.98676	−4.33433	4.22047	−3.08288	0.99090
1.8457	25.4152	1.81442	−3.91407	3.75891	−2.75288	0.89204
2.1014	26.6985	1.65886	−3.49263	3.18967	−2.24892	0.70450
2.3872	28.0171	1.51831	−3.16521	2.86331	−2.03308	0.64564
2.6661	29.2065	1.39140	−2.86538	2.52902	−1.77394	0.56060
3.0217	30.5980	1.24760	−2.55726	2.23329	−1.58084	0.50998
3.3085	31.6426	1.14481	−2.36198	2.06650	−1.46999	0.47821
3.5697	32.5679	1.05509	−2.18428	1.87456	−1.30535	0.41888
			$YbCl_3$			
0.096912	9.1514	3.72073	−8.93535	9.87395	−7.52890	2.45243
0.24755	11.3108	3.56569	−8.67026	10.23166	−8.26455	2.82489
0.42932	13.3807	3.27677	−7.73270	8.78119	−6.91248	2.32044
0.63692	15.3674	2.99089	−6.89964	7.53210	−5.74325	1.87457
0.85624	17.1825	2.70568	−6.07670	6.35814	−4.74924	1.53378
1.1438	19.2440	2.40711	−5.32097	5.45016	−4.07661	1.32966
1.4468	21.1667	2.13162	−4.59190	4.48909	−3.28996	1.06504
1.7552	22.9278	1.90633	−4.01084	3.74333	−2.64519	0.82609
2.0830	24.6418	1.71055	−3.54536	3.27709	−2.35764	0.75758
2.4142	26.2318	1.54115	−3.13797	2.81755	−1.99421	0.63350
2.7644	27.7682	1.38399	−2.77984	2.44602	−1.73233	0.55810
3.1214	29.1945	1.23672	−2.44867	2.06451	−1.42040	0.45306
3.4947	30.5624	1.11046	−2.24287	1.95139	−1.38655	0.46004

Table VIII. Matrix Coefficients, B_{ij}, Corresponding to Equation 4

j	B_{0j}	$B_{1j} \times 10$	$B_{2j} \times 10^3$	$B_{3j} \times 10^5$	$B_{4j} \times 10^7$	$B_{5j} \times 10^9$
			$SmCl_3$			
0	8.79272	3.633290	−9.207126	10.581492	−8.498357	2.845232
1	5.68926	1.719658	−1.688217	3.257708	−2.437776	0.820360
2	8.84064	−4.750366	9.697633	−15.967735	13.899013	−4.856224
3	−4.45278	2.530876	−5.316871	9.771461	−9.019395	3.217975
4	0.84321	−0.439665	0.905332	−1.873181	1.810152	−0.656795
			$GdCl_3$			
0	12.51134	3.214004	−9.104461	10.601625	−8.002207	2.302221
1	0.82659	2.356689	−2.465442	5.645571	−7.683728	4.432602
2	16.15518	−5.954562	12.111485	−22.385991	24.727501	−11.411894
3	−9.12490	3.436574	−7.368226	14.857264	−16.845767	7.689722
4	1.80696	−0.654865	1.420572	−3.130848	3.672479	−1.686999
			$DyCl_3$			
0	11.69037	3.265827	−8.568245	8.328155	−5.039354	1.027088
1	1.18948	2.261705	−3.387633	9.019313	−11.661217	5.867764
2	16.07697	−5.629731	11.661891	−21.430774	22.926090	−10.074390
3	−8.41597	3.074596	−6.361837	11.992867	−12.856155	5.589461
4	1.51815	−0.561024	1.106200	−2.187188	2.402396	−1.053455
			$ErCl_3$			
0	9.03266	3.466844	−8.904948	9.300320	−6.557997	1.867643
1	4.79945	1.954430	−3.187235	7.658626	−8.668782	3.906149
2	10.60908	−5.287963	11.810209	−20.743802	20.423988	−8.170145
3	−4.90249	2.887697	−6.497133	11.772823	−11.746071	4.684687
4	0.75779	−0.526137	1.130281	−2.138067	2.192527	−0.883361
			$YbCl_3$			
0	5.63238	3.712794	−9.978995	11.994744	−9.905657	3.459956
1	10.11309	1.354181	0.537387	−2.032094	3.282440	−1.700918
2	3.12236	−4.540127	6.816343	−7.660794	4.416068	−0.734692
3	−0.50469	2.463077	−3.600014	4.181916	−2.521691	0.429468
4	−0.13014	−0.439087	0.528115	−0.560368	0.284882	−0.006570

Table IX. Parameters in Masson's Equation, $\phi_V = \phi_V^* + S_V^* m^{1/2}$

t, °C	$SmCl_3$	$GdCl_3$	$DyCl_3$	$ErCl_3$	$YbCl_3$
			ϕ_V^*, ml/mol		
5	8.45	11.53	10.52	8.55	6.20
10	9.93	12.84	11.92	9.99	7.69
15	11.05	13.79	12.95	11.07	8.80
20	11.86	14.46	13.68	11.84	9.61
25	12.42	14.87	14.15	12.35	10.15
30	12.75	15.07	14.40	12.64	10.46
35	12.89	15.09	14.45	12.74	10.59
40	12.86	14.94	14.34	12.67	10.54
45	12.68	14.66	14.08	12.45	10.33
50	12.36	14.24	13.68	12.08	9.98
55	11.91	13.69	13.14	11.59	9.50
60	11.34	13.03	12.49	10.97	8.89
65	10.66	12.26	11.72	10.23	8.16
70	9.87	11.37	10.84	9.37	7.32
75	8.97	10.38	9.85	8.41	6.37
80	7.98	9.30	8.76	7.34	5.31
			S_V^*		
5	12.61	11.76	12.68	12.99	13.30
10	12.10	11.30	12.12	12.42	12.72
15	11.75	10.99	11.72	12.00	12.29
20	11.52	10.80	11.44	11.71	11.98
25	11.40	10.71	11.27	11.52	11.79
30	11.37	10.70	11.19	11.42	11.68
35	11.41	10.77	11.19	11.39	11.65
40	11.52	10.89	11.25	11.43	11.68
45	11.69	11.07	11.36	11.52	11.78
50	11.90	11.30	11.54	11.67	11.92
55	12.17	11.57	11.75	11.87	12.12
60	12.48	11.88	12.02	12.11	12.36
65	12.84	12.24	12.33	12.34	12.65
70	13.23	12.63	12.68	12.72	12.98
75	13.66	13.07	13.07	13.09	13.36
80	14.12	13.53	13.50	13.50	13.77

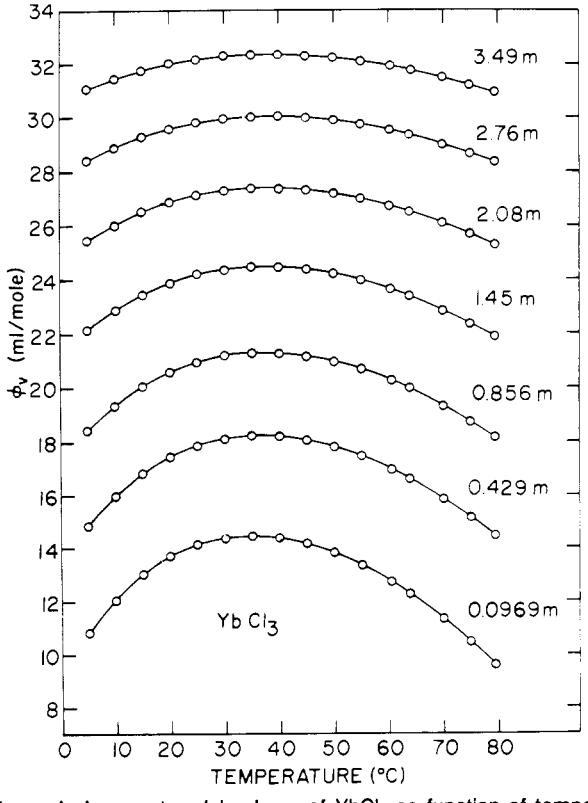

Figure 1. Apparent molal volume of $YbCl_3$ as function of temperature. Circles, experimental; lines, Equation 3

Table X. Some Properties at Infinite Dilution

t, °C	$LaCl_3$	$PrCl_3$	$NdCl_3$	$SmCl_3$	$GdCl_3$	$DyCl_3$	$ErCl_3$	$YbCl_3$
				$\overline{V}_2^0$, ml/mol				
5	11.74	7.30	6.52	7.94	10.60	9.84	7.90	5.55
25	14.54	10.40	9.66	10.68	12.82	12.16	10.37	8.16
50	13.69	9.33	8.69	9.48	11.07	10.37	9.35	6.61
75	8.39	4.77	4.27	4.92	6.02	5.27	3.71	1.65
80	7.07	3.50	3.03	3.66	4.64	3.91	2.35	0.32
				$\overline{E}_2^0$, ml mol^{-1} deg^{-1}				
5	0.255	0.292	0.291	0.263	0.238	0.246	0.252	0.260
25	0.036	0.046	0.049	0.036	0.011	0.013	0.020	0.026
50	−0.107	−0.118	−0.114	−0.120	−0.139	−0.143	−0.113	−0.137
75	−0.248	−0.243	−0.237	−0.241	−0.264	−0.262	−0.260	−0.256
80	−0.281	−0.265	−0.259	−0.262	−0.289	−0.282	−0.282	−0.276
				$\overline{E}^0$ (RE^{3+}), ml mol^{-1} deg^{-1}[a]				
25	−0.102	−0.092	−0.089	−0.102	−0.127	−0.125	−0.118	−0.112
				T_{max}, °C[b]				
	28.8	30.6	30.9	29.8	27.1	26.7	27.7	28.2

[a] Based on $\overline{E}^0(Cl^-)$ = 0.046 ml mol^{-1} deg^{-1} (*10*). [b] Temperature of maximum in $\overline{V}_2^0$.

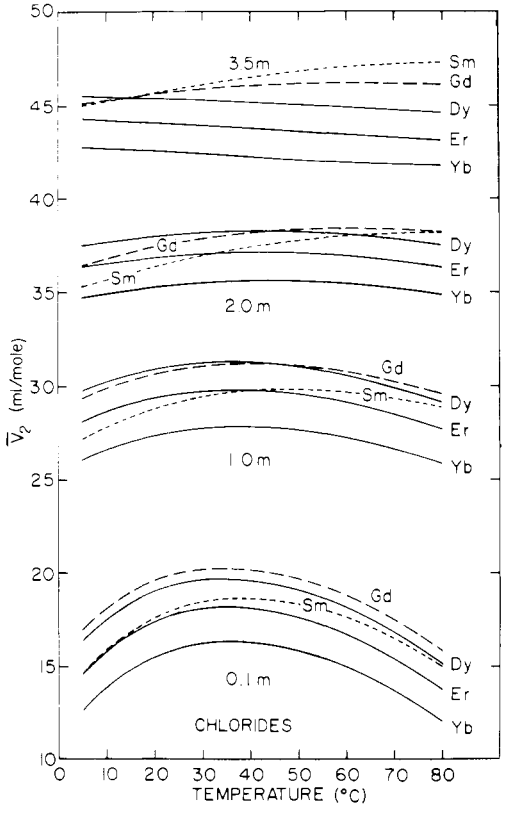

Figure 2. Partial molal volume of some rare earth chlorides as function of temperature. From Equation 4

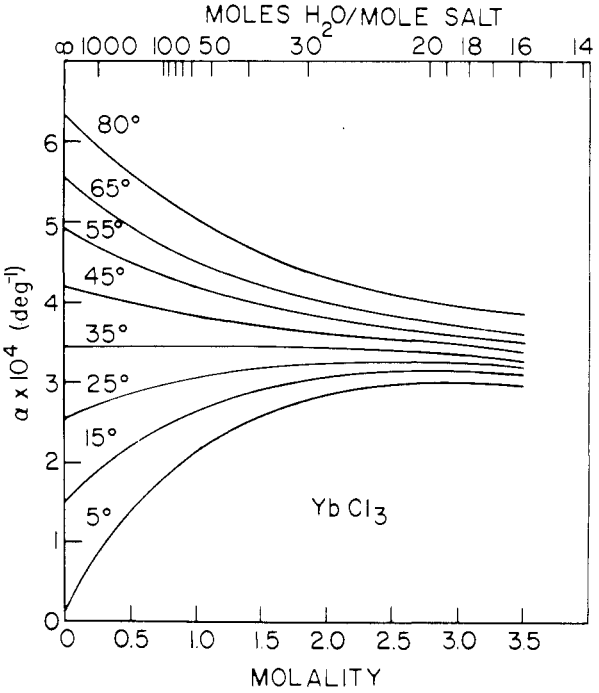

Figure 3. Coefficients of thermal expansion of $YbCl_3$ solutions as function of molality. From Equation 4

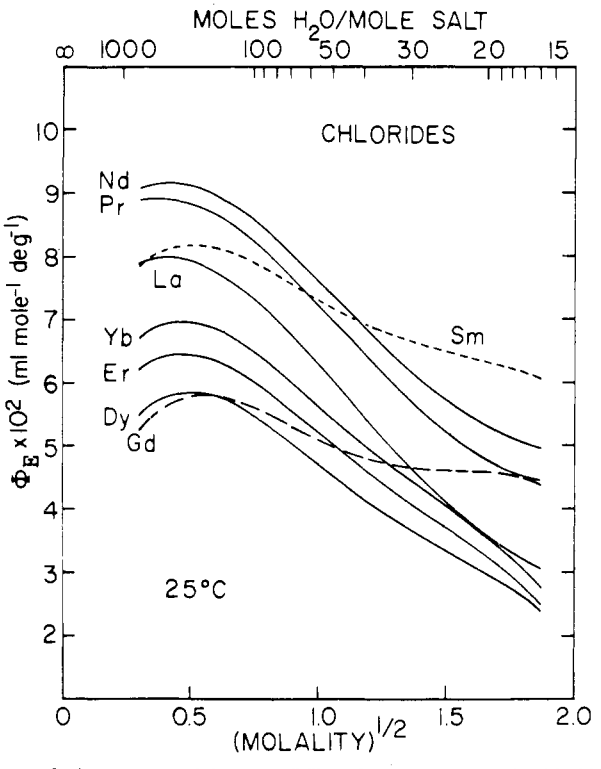

Figure 4. Apparent molal expansibility of some rare earth chlorides as function of $m^{1/2}$ at 25°C. From Equation 4

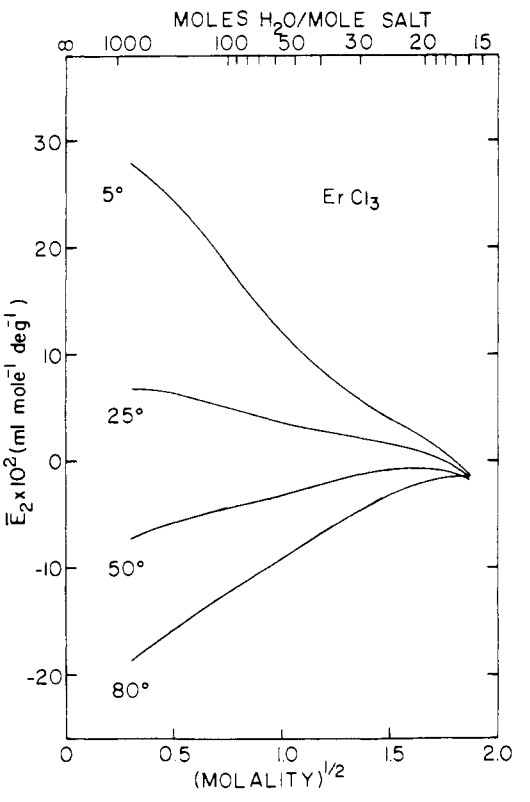

Figure 6. Partial molal expansibility of $ErCl_3$ as function of $m^{1/2}$. From Equation 4

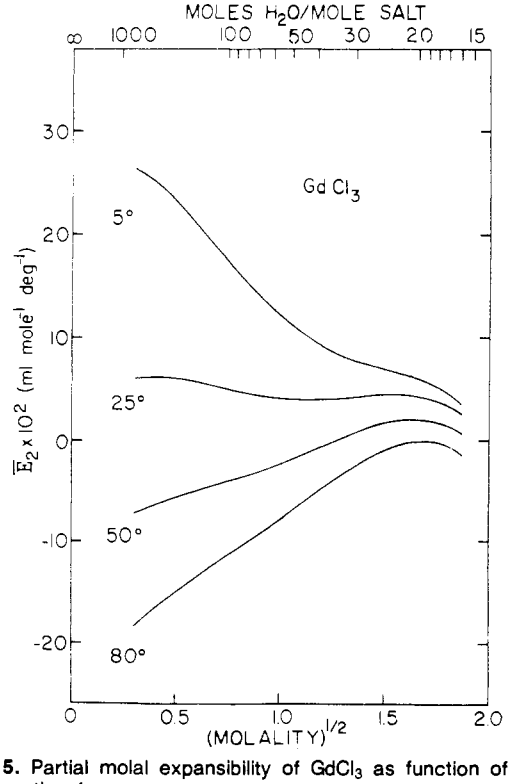

Figure 5. Partial molal expansibility of $GdCl_3$ as function of $m^{1/2}$. From Equation 4

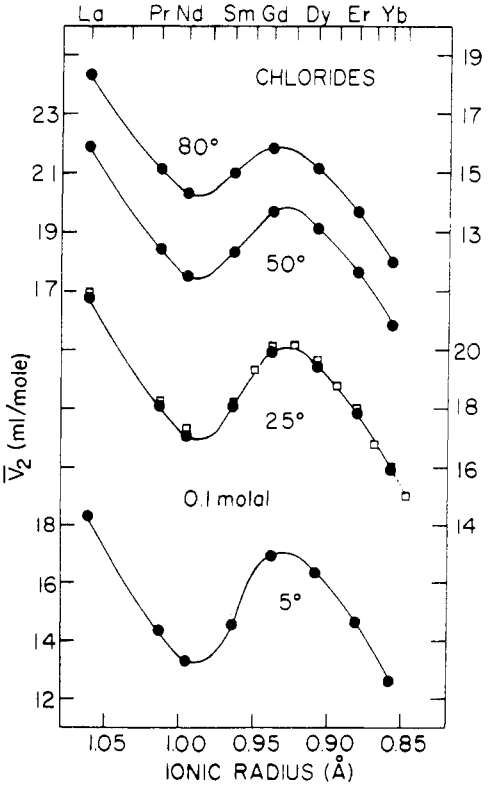

Figure 7. Partial molal volumes of some rare earth chlorides as function of ionic radius at 0.1*m*. Circles, Equation 4; squares, from Spedding et al. (*18*)

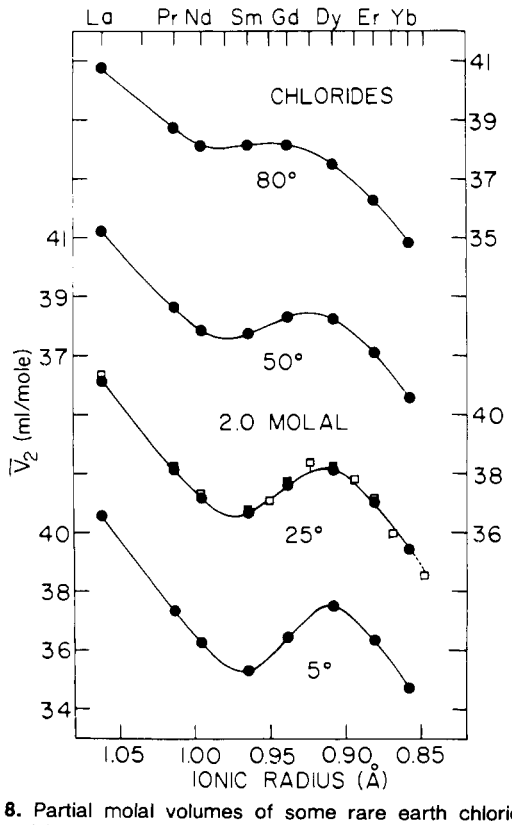

Figure 8. Partial molal volumes of some rare earth chlorides as function of ionic radius at 2*m*. Circles, Equation 4; squares, from Spedding et al. (*18*)

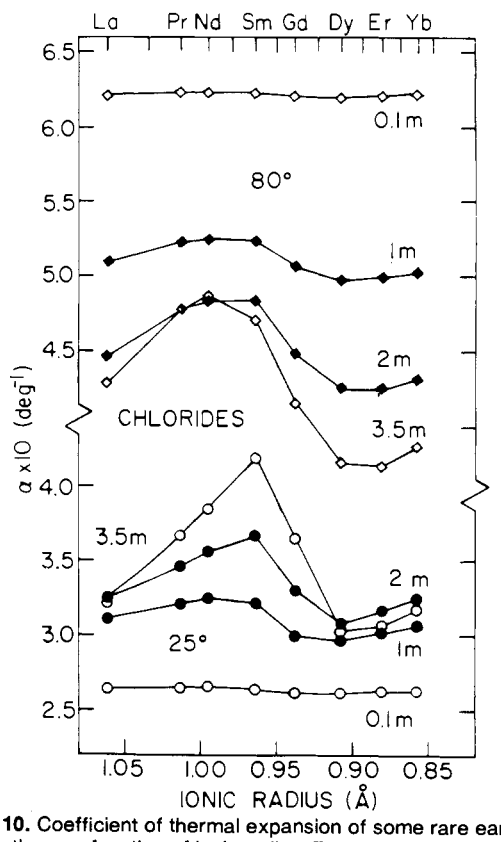

Figure 10. Coefficient of thermal expansion of some rare earth chloride solutions as function of ionic radius. From Equation 4

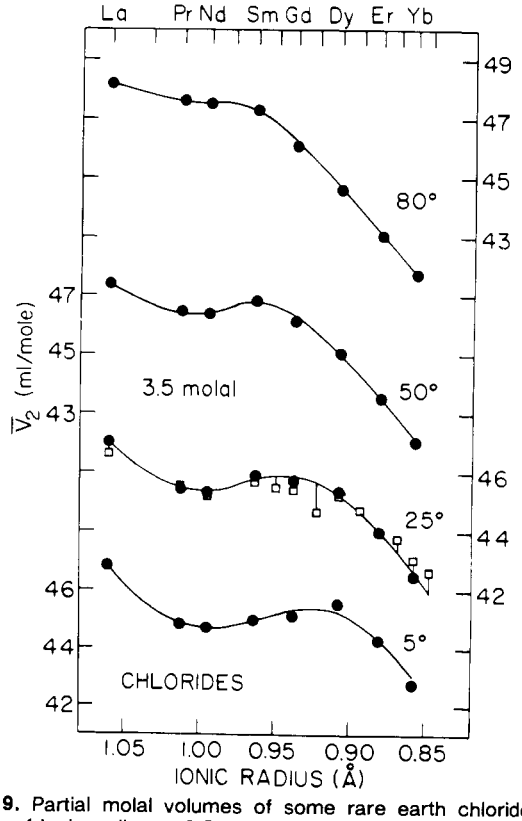

Figure 9. Partial molal volumes of some rare earth chlorides as function of ionic radius at 3.5*m*. Circles, Equation 4; squares, from Spedding et al. (*18*)

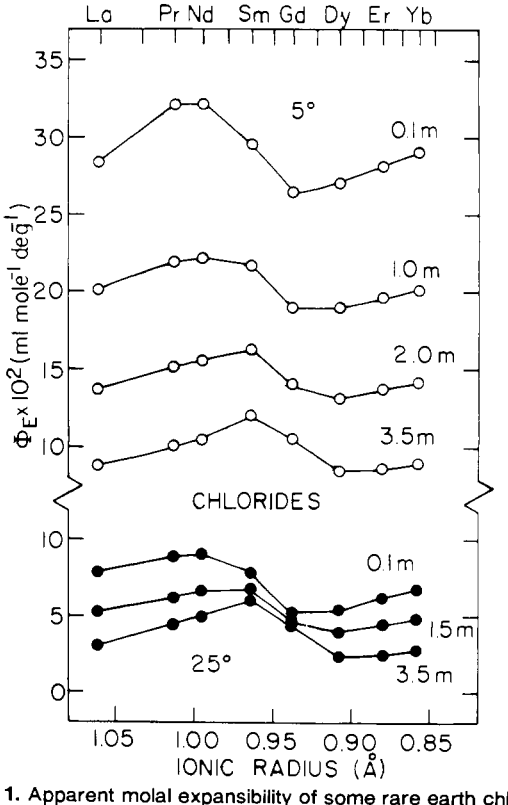

Figure 11. Apparent molal expansibility of some rare earth chlorides as function of ionic radius. From Equation 4

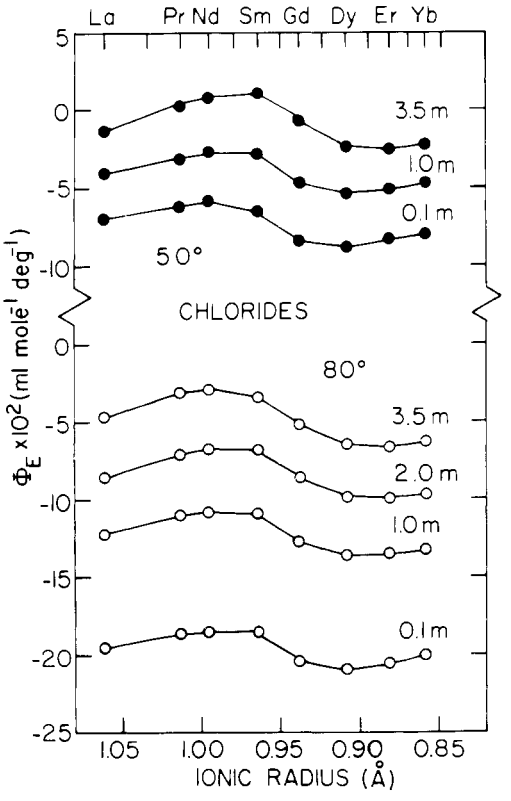

Figure 12. Apparent molal expansibility of some rare earth chlorides as function of ionic radius. From Equation 4

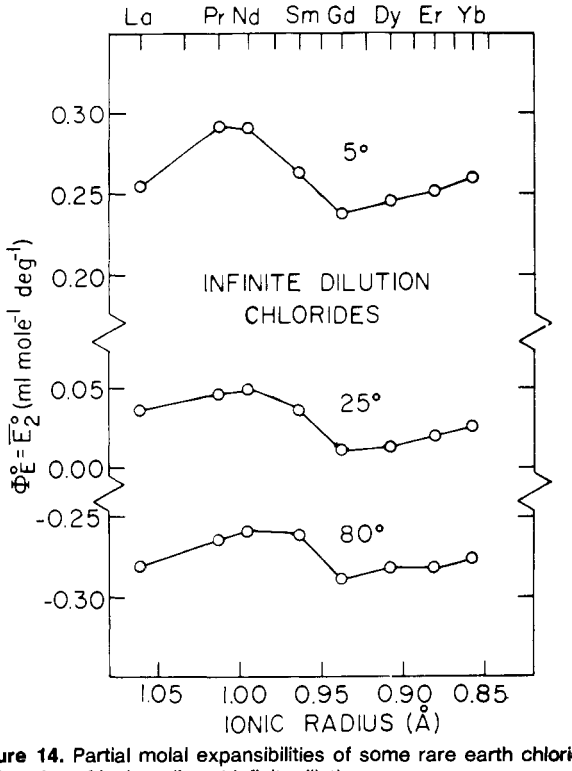

Figure 14. Partial molal expansibilities of some rare earth chlorides as function of ionic radius at infinite dilution

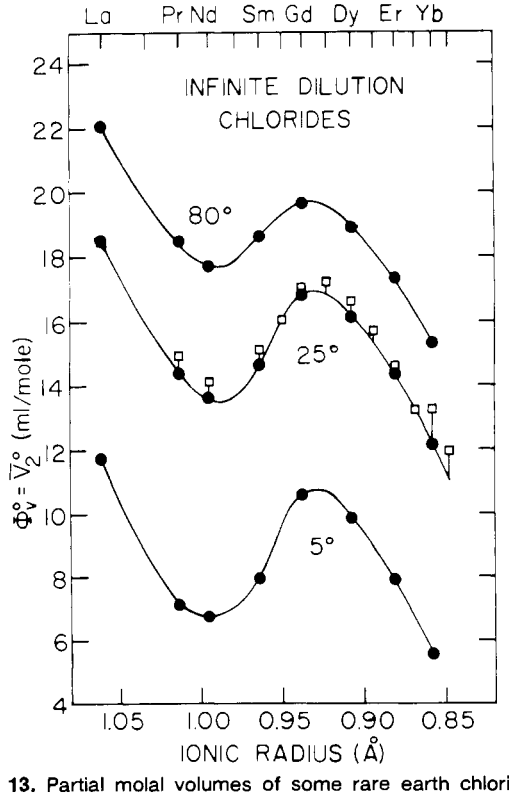

Figure 13. Partial molal volumes of some rare earth chlorides as function of ionic radius at infinite dilution. Circles, Redlich-Meyer equation extrapolation; squares, from magnetic float measurements (*14*)

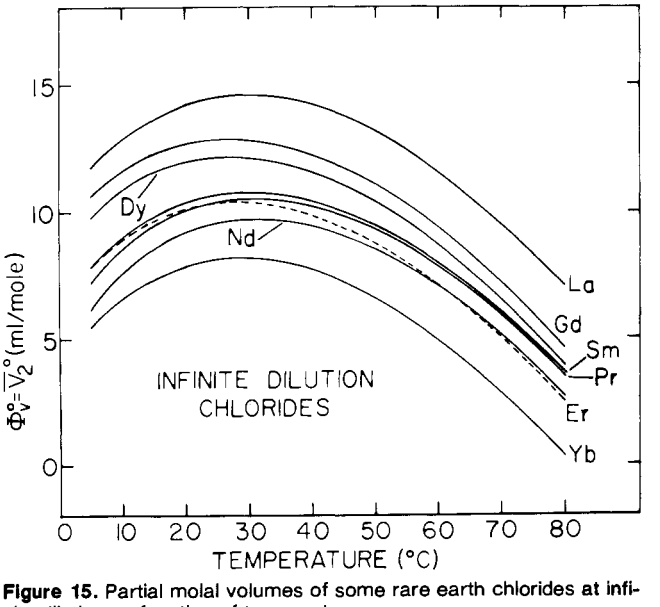

Figure 15. Partial molal volumes of some rare earth chlorides at infinite dilution as function of temperature

that the $\bar{V}^0$ (ion) are smaller (algebraically) than those of the divalent and monovalent ions, and $\bar{V}^0$ (ion) for the rare earth ions also decrease with decreasing ionic radius across the series as expected (for a given inner sphere hydration number). These considerations, therefore, qualitatively account for the overall decrease in $\bar{V}_2^0$ from La to Nd and Tb to Lu, shown in Figure 13, being due to the increase in surface charge density with decreasing radius. Within this framework, the expulsion of an electrostricted inner sphere water molecule results in a decrease in the total electrostriction and an increase in $\bar{V}_2^0$ between Nd and Tb (*14, 15*).

Millero (*10*) has attempted to extend these concepts to include variation with temperature. He showed that the $\bar{E}^0$ (ion) for the divalent alkaline earth chloride solutions are in agreement with the theoretical values predicted by the temperature derivative of the Drude-Nernst (*1*) equation, which requires that $\bar{E}^0$ (ion) decrease with increasing charge and decreasing radius as was the case for $\bar{V}^0$ (ion). However, the $\bar{E}^0$ (ion) for the monovalent cations (except Li^+) increased with decreasing ionic radius, opposite the trend expected. Combining the value for $\bar{E}^0$ (Cl^-) = 0.046 ml mol^{-1} deg^{-1} used by Millero, and the value of $\bar{E}_2^0$ in Table X for the rare earth chlorides, we find $\bar{E}^0$ (ion) to be in the range −0.09 to −0.13 ml mol^{-1} deg^{-1} (Table X). These are indeed smaller (algebraically) than for the divalent (−0.01 to −0.10 ml mol^{-1} deg^{-1}) and monovalent (−0.01 to +0.03 ml mol^{-1} deg^{-1}) cations, in agreement with the expectations in regard to increasing charge. However, except for the hydration change, the trend with decreasing ionic radius is clearly an increase in $\bar{E}^0$ (ion) for the rare earth ions (see Figure 14, and at finite concentrations, Figures 11 and 12). This trend with radius is the same as for the monovalent cations, but opposite the trend in the divalent cations and the trend predicted by simple theory.

The temperature where $\bar{V}_2^0$ goes through a maximum, T_{max} (shown in Figure 15 and listed in Table X), clearly is related to the behavior of $\bar{E}^0$ (ion) for the rare earth chloride solutions. T_{max} generally occurs at lower temperatures with increasing charge on the cation (*2, 7, 9*), suggesting a surface charge density dependence, i.e., T_{max} = 60° (NaCl), 44° ($CaCl_2$), and 27–31°C for the rare earth chloride solutions. However, as with $\bar{E}^0$ (ion), T_{max} increases with decreasing radius in the rare earth series (except for the hydration change).

Intuitively, one would of course expect the electrostricted region around a highly charged ion to have a smaller expansibility than the bulk solvent in the case of the nonstructured, continuous dielectric solvent approximation. And furthermore, this decrease should be greater for smaller ions and ions of greater charge. This model is clearly not sufficient in the case of aqueous solutions, where the unique structural character of the solvent gives rise to distinctive behavior in the thermal expansion properties.

The reason for the general increase in $\bar{E}_2^0$ across the rare earth series, for a given inner sphere water coordination, is not known at this time. However, the displacement of this trend in $\bar{E}_2^0$ between Nd and Tb (dilute solutions) in analogy with similar two-series effects in the other thermodynamic properties suggests that it is due to the displacement of the equilibrium between the two coordination numbers in the region of Nd to Tb. Finally, the multilayer hydration model reviewed by Millero (*9*) includes a disordered region between the electrostricted region and the bulk solvent. Since the size of the electrostricted region of the rare earth ion increases from La to Lu as shown by conductivity measurements (*17*), the disordered region may also be increasing in size across the series. The increase in $\bar{E}_2^0$ across the rare earth series may be related to this increase in size of the disordered region and the unique nature of the solvent structure.

Acknowledgment

The authors thank the Ames Laboratory Rare Earth Separation Group for furnishing the oxides. They are also indebted to J. A. Rard for many helpful discussions.

Literature Cited

(1) Drude, P., Nernst, W., *Z. Phys. Chem. (Frankfurt)*, **15,** 79 (1894).
(2) Dunn, L. A., *J. Solution Chem.*, **3,** 1 (1974).
(3) Gildseth, W. M., Habenschuss, A., Spedding, F. H., *J. Chem. Eng. Data*, **17,** 402 (1972).
(4) Gildseth, W. M., Habenschuss, A., Spedding, F. H., *ibid.*, **20,** 292 (1975).
(5) Habenschuss, A., PhD dissertation, Iowa State University, Ames, Iowa, 1973.
(6) Harned, H. S., Owen, B. B., "The Physical Chemistry of Electrolytic Solutions", 3rd ed., Reinhold, New York, N.Y., 1958.
(7) Jones, G., Taylor, E. F., Vogel, R. C., *J. Am. Chem. Soc.*, **70,** 966 (1948).
(8) Masson, D. O., *Phil. Mag., Ser., 7*, **8,** 218 (1929).
(9) Millero, F. J., in "Water and Aqueous Solutions", R. A. Horne, Ed., Chaps. 13, 14, Wiley-Interscience, New York, N.Y., 1972.
(10) Millero, F. J., *J. Phys. Chem.*, **72,** 4589 (1968).
(11) Owen, B. B., White, J. R., Smith, J. S., *J. Am. Chem. Soc.*, **78,** 3561 (1965).
(12) Rard, J. A., Spedding, F. H., *J. Phys. Chem.*, **79,** 257 (1975).
(13) Redlich, O., Meyer, D., *Chem. Rev.*, **64,** 221 (1964).
(14) Spedding, F. H., Cullen, P. F., Habenschuss, A., *J. Phys. Chem.*, **78,** 1106 (1974).
(15) Spedding, F. H., Pikal, M. J., Ayers, B. O., *ibid.*, **70,** 2440 (1966).
(16) Spedding, F. H., Rard, J. A., *ibid.*, **78,** 1435 (1974).
(17) Spedding, F. H., Rard, J. A., Saeger, V. W., *J. Chem. Eng. Data*, **19,** 373 (1974).
(18) Spedding, F. H., Saeger, V. W., Gray, K. A., Boneau, P. K., Brown, M. A., DeKock, C. W., Baker, J. L., Shiers, L. E., Weber, H. O., Habenschuss, A., *ibid.*, **20,** 72 (1975).
(19) Spedding, F. H., Shiers, L. E., Brown, M. A., Baker, J. L., Gutierrez, L., Habenschuss, A., *J. Phys. Chem.* (May 1975).
(20) Spedding, F. H., Shiers, L. E., Brown, M. A., Derer, J. L., Swanson, D. L., Habenschuss, A., *J. Chem. Eng. Data*, **20,** 81 (1975).
(21) Spedding, F. H., Shiers, L. E., Rard, J. A., *ibid.*, p 88.
(22) Templeton, D. H., Dauben, C. H., *J. Am. Chem. Soc.*, **76,** 5237 (1954).

Received for review May 7, 1975. Accepted July 22, 1975. Report prepared for the U.S. Energy Research and Development Administration under Contract No. W-7405-eng-82, and based in part on the PhD dissertation of A.H. (1973) submitted to the Graduate Faculty of Iowa State University, Ames, Iowa. By acceptance of this article, the publisher and/or recipient acknowledges the U.S. Government's right to retain a nonexclusive, royalty-free license in and to any copyright covering this paper.